CARBON DIOXIDE EXCHANGE OVER A SUBARCTIC WETLAND

When I couldn't do it on my own,
your strength and confidence held me steadfast.

This work is dedicated to my family.

c.s.

SUMMERTIME CARBON DIOXIDE EXCHANGE OVER A SUBARCTIC SEDGE WETLAND

By

CHERYL PATRICIA SCHREADER, Hon. B.Sc.

A Thesis

Submitted to the School of Graduate Studies

in Partial Fulfillment of the Requirements

for the Degree

Master of Science

McMaster University

November 1995

MASTER OF SCIENCE (1995)
(Geography)

McMASTER UNIVERSITY
Hamilton, Ontario

TITLE: Summertime Carbon Dioxide Exchange over a Subarctic Sedge Wetland

AUTHOR: Cheryl Patricia Schreader, Hon. B.Sc. (Trent University)

SUPERVISOR: Professor W.R. Rouse

NUMBER OF PAGES: xiii, 101

ABSTRACT

Measurements of net ecosystem carbon dioxide fluxes were made over a sedge fen, Churchill, Manitoba during the summertime period, 1994. This period, when compared to 50 year records (1943 to 1993), was warm and dry. The mean daily temperature was 2 °C warmer than normal. Total precipitation for the summertime period was 45% less than normal, with 56% of the events occurring during the month of August. The water table was generally 0.30 m below the surface and periodically as deep as 0.44 m. The active layer reached a depth of 1.12 m by the end of the measurement period. The growing season for sedge extended from June 23 to August 8.

Using atmospheric gradient techniques, the total net ecosystem flux of carbon dioxide over the measurement period was determined. The total summertime flux was positive indicating that the tundra is losing more carbon dioxide through respiration than it is gaining via photosynthesis. There is still a substantial loss during the period of active photosynthesis. In fact, almost one half of the total carbon dioxide efflux occurred during the period of active growth.

It is hypothesized that warmer soil temperatures and better aerated soil conditions are more conducive to decomposition, therefore resulting in a larger absolute respiration flux relative to photosynthesis. This is in accordance with several other high latitude studies.

ACKNOWLEDGEMENTS

I admit that I am the type of person that generally draws upon the support of many people. I surround myself with as many confident, knowledgable, fun, caring people that I possible can. For this reason, my acknowledgements are never-ending but nonetheless very important.

The person most responsible for this research is Dr. Wayne Rouse. His boisterous enthusiasm both in the field and in the lab is contagious. His support, knowledge and curiosity have been both motivating and stimulating. Thank you for a wonderful experience.

I have quickly come to realize that, although this research opportunity was provided by a higher power, there is one single person, without whom this project would not be possible. His unending and sometimes tiresome diligence, dedication, patience and outstanding field and computer expertise have been nothing less than paramount in the success of this research. Dale, you have been a fantastic co-worker and have become a great friend. I can't say enough.

The field work in this project was fairly intensive and demanded many hands. I would like to offer many thanks to my hardy field assisstant, Derek Barber. Even throughout the most tedious of tasks, and the harshest of working of environments (weather included), I was always greeted with "Hey, sunshine". Although, I'm sure that outside of my company, I was referred to with less enthusiasm . I would also like to thank Bruce "Brucé" Wurlete for his volunteered help in the soil chamber measurements during both scorching sun and treacherous wind and rain. Although not

included in this project, instrumentation for soil respiration was provided by Dr. Darwin Coxson. I refuse to believe that our efforts were in vain. Your insights into the biological "side" were much appreciated. Thank you also to Dr. Peter Lafleur whose guidance and inquisitive mind have always been an asset in my research endeavors.

Research in the north can be quite difficult, but thanks to the staff of the Churchill Northern Studies Centre, my summer-long visits have always been enjoyable. Thank you Kevin, Mike, Stacey, Barb Cliff, Lindy and of course, Joan. And to Nicole...what can I say? Churchill will never be the same.

Back at the ranch, life and work as I know it, would not be possible without a fantastic crew of friends. My warmest gratitude goes out to Kim and Pierre, Dale and other Climo's (Tim and Rich), Ros, Mark, Andrea, Penn, Steve, Shannon and Julian and there's just so many others. Thanks for the friendships, the support and all the necessary distractions.

I know that words will not do justice in thanking the next group of people. You could call them my family away from home. Thank you to Aunt Earla and Uncle Jim, Sue and Ian, and Chris. I can't say how much I appreciate the home enviroment you provided during my last few months. From the home-cooked meals, a warm bed, all the rides, to all the love, support and guidance you have given me. Thank you so much, I will never forget it.

I could not complete these acknowledgements without including the support of one very special person. Thank you Joe, for having confidence in me, for being a wonderful friend and for

helping me realize that there is life outside of academia. Now I can go find it.

And I think I owe the largest part of this personal achievement to the people closest to me, my family. Your unwavering love and support over the past few years has given me the confidence to face challenges with courage and to live every day to the fullest. "Carpe diem"! I have learned not only 'academics' in this achievement, but respect for hard work, for others, for life and for myself. I could not have done it without you. Thank you.

Financial support was provided by National Science and Engineering Research grants to WRR and by a Northern Study Training grant to CS.

TABLE OF CONTENTS

LIST OF FIGURES

LIST OF TABLES

CHAPTER 1

Introduction and Literature Review

1.1 Nature of the research

It is predicted that global surface temperatures will increase in response to increases in atmospheric CO_2, with the largest increases expected for northern regions during winter. The integrity of northern regions is highly sensitive to changes in temperature because of the dominance of ice, snow and permafrost in these environments. Owing to their large areal extent and abundant carbon reserves, it is essential to quantify the role of these regions in the carbon cycle on a long term basis to successfully model global response to climate change. Equally important is the determination of environmental controls on the CO_2 budget.

This paper reports on climatological conditions and net CO_2 fluxes for a 75 day summertime period (June, July and August), 1994. Attempts are made to quantify the influence of plant phenology, water table position and temperature on field measurements of CO_2 fluxes. The study site is a sedge dominated fen located within the Hudson Bay Lowland near Churchill, Manitoba. This landscape is representative of an extensive band of high subarctic wetland which extends from the north-western corner of James Bay, north-west along the coast of Hudson Bay and farther north-west towards Inuvik (Zoltai and Pollet, 1983). The results are part of a longer term CO_2 monitoring program pioneered by Burton

et al. (1994). This program is the first field intensive CO_2 study to be initiated in the Churchill region.

1.2 Scientific Impetus and Background

Changes in the atmospheric concentrations of CO_2 have been shown to be dynamic over many time-scales, from months, years, decades (Bacastow and Keeling, 1981) and centuries (Neftel *et al.*, 1985) to millennium (Neftel *et al.*, 1982) and tens and hundreds of millennia (Neftel *et al.*, 1982; Barnola *et al.*, 1987). For example, over millennia, CO_2 has been implicated in triggering the onset and completion of ice-ages (Hays *et al.*, 1976). Over centuries, *e.g.* the period from the 18th century to now, the measurements of CO_2 concentration reflect the increased anthropogenic influence on atmospheric CO_2 (Friedli *et al.*, 1986). The monthly variations of CO_2 appear to provide a strong signal of the fluxes of CO_2 between the terrestrial biosphere and the atmosphere (Pearman and Hyson, 1980; Keeling, 1988). At a range of time-scales therefore, changes in the atmospheric concentration of CO_2 signal a wide range of activities by the global biosphere, the interpretation of which requires an understanding of the feedback responses between the biosphere and atmospheric CO_2.

CO_2 concentrations have been rapidly increasing in the earth's atmosphere during the last 2 centuries from a benchmark of approximately 260 ppm (Trabalka, 1985). Results from monitoring networks at Mauna Loa in mid-Pacific, the South Pole and from Point Barrow,

Alaska all show the same thing. In 27 years, the atmospheric CO_2 concentrations have risen from ~ 315 ppm in 1958 to ~ 345 ppm in 1985 (Billings, 1987). This atmospheric increase in CO_2 represents an amount of CO_2 equivalent to 58% of the releases from fossil fuel combustion during that same period of time (Rotty and Masters, 1985). More recent data from Mauna Loa (Conway *et al.*, 1988) illustrates that fluctuations are more pronounced in the northern hemisphere due to the size of the continents (Figure 1.1).

Natural oscillations in CO_2 concentrations in the atmosphere have occurred during the last million years (Gammon *et al.*, 1985). These cycles exhibit values ranging between ~200 ppm during cold glacial periods and ~270 ppm during warm interglacials (Billings, 1987). However, there have not been any concentrations of CO_2 in the atmosphere comparable to those at present since the Tertiary (Billing, 1987). The increases in CO_2 witnessed during the last decade have been far larger and have occurred at a much faster rate than at any other time in history.

It is predicted that as early as the middle of the next century, mean surface temperatures could increase more than at any other time during the past several million years. With continued use of fossil fuels and the resultant increase in atmospheric CO_2, Global Circulation Model (GCM) simulations predict that the global average temperature could rise between 1.5 and 4.5°C (Billings, 1987). The Intergovernmental Panel for Climate Change (1990) predicted that the globe may warm an average of 1°C in the next 35 years and by 3°C

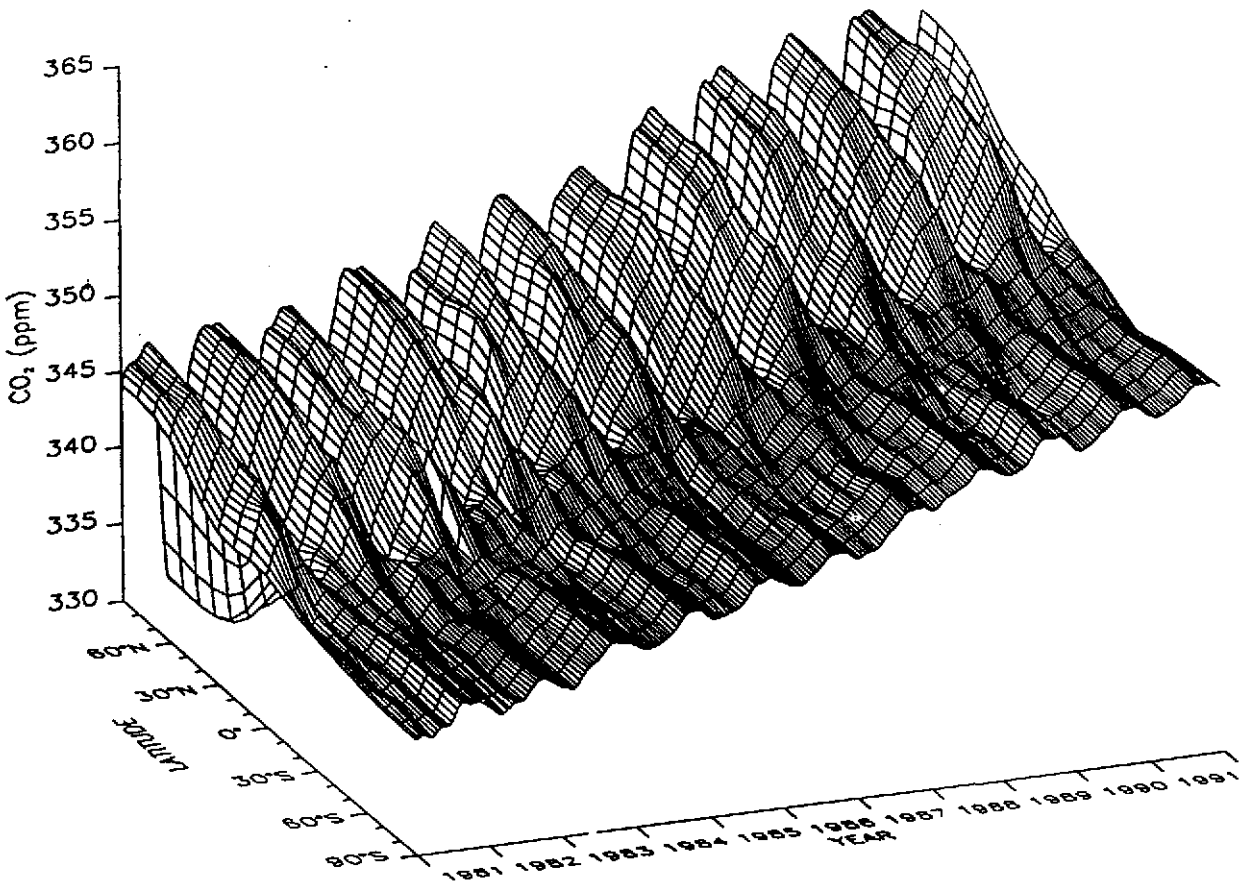

Figure 1.1: Seasonal fluctuations of atmospheric CO_2 during the years 1981 to 1991 (after Conway *et al.*, 1988).

by the year 2100 in response to increases in greenhouse gases. CO_2 is the most critical greenhouse gas being emitted through human activity. It is responsible for ~60% of the extra greenhouse effect thus far and is likely to account for 50 to 75% of the future increase (Ministry of Supply and Service, 1991). This transition will be unlike any previous climate change in two important ways. First, it will occur much more rapidly than in the past and second, it will not be naturally induced. Today's warming could occur 100 times faster than the warming at the end of the last ice age (Ministry of Supply and Service, 1991).

The role of natural terrestrial systems in ameliorating or contributing to increased CO_2 concentrations has not been studied to any appreciable extent. Northern regions are particularly interesting since arctic and subarctic ecosystems are estimated to contain 21% of the total carbon pool, primarily in the form of peat (Miller *et al.*, 1983; Miller, 1981). These regions are also expected to undergo the greatest climatic changes in response to the increases in global CO_2. The importance of permafrost, ice and snow in controlling Arctic ecosystem processes makes these regions particularly sensitive to warming. Solomon *et al.* (1985) suggest that mean temperatures in high latitudes could rise as much as 9°C with most of the warming trend during the winter months. Manabe and Stouffer (1980) and Wigley *et al.* (1980) predicted annual increases in temperature of up to 11°C for Arctic regions with summer increases ranging from 1.5 to 4.5°C. Oechel *et al.* (1993) have predicted surface temperature increases of 4°C in the summer and as much as 17°C during the winter in high northern regions for a doubling of CO_2.

There are basically two schools of thought on how northern regions may react to such

changes. One opinion is that because these regions of cold acidic soils, underlain by permafrost are capable of such considerable carbon storage, they may act as a partial buffer to changes in atmospheric CO_2 (Hilbert *et al.*, 1987). Billings *et al.* (1982) however, suggest that with such large increases in temperature, these existing large carbon pools may be liberated into the atmosphere.

The world's standing biomass contains ~800 Gt C and the world's soils contain another 1500 Gt C (Mellilo *et al.*, 1990). Northern ecosystems alone contain up to 455 Gt C in the soil active layer and the upper levels of the permafrost. This translates into ~30% of the world soil store and up to 60% of the ~750 Gt currently in the atmosphere as CO_2. Billings (1987) notes that this would only be a minimum figure because much of the carbon is immobilized in permafrost and he stresses the role of permafrost in maintaining the integrity of the tundra and its carbon balance. An estimated 14% of the earth's terrestrial stored carbon is found as peat and dead organic matter in Arctic tundra ecosystems (Post et al., 1982) which contain more than 50 Gt C below ground as dead organic matter. Over 97% of the total carbon in the tundra ecosystem is stored in peaty soil and in the carbon in the living part of the system, with ~81% being held in the roots and rhizomes of the dominant grasses and sedges. Therefore, except for carbon fixation, the tundra is predominantly a below ground system (Billings, 1987).

Carbon accumulation rates can also be quite significant. Reported accumulation rates for wet tundra vary from 10 - 20 g C m^{-2} yr^{-1} to 40 - 120 g C m^{-2} yr^{-1} (Tiezen, 1978; Coyne and Kelly, 1978; Miller *et al.*, 1983) while tussock tundra accumulation rates are slightly

lower (23 g C m^{-2} yr^{-1}) (Chapin *et al.*, 1980; Coyne and Kelly, 1975). In the historical and recent geological past, rates of carbon accumulation in tundra regions worldwide have been ~0.1 - 0.3 Gt C yr^{-1} (*from* Oechel *et al.*, 1993).

1.3 Carbon Cycling

To investigate the effects of climate change on the carbon balance of a particular region, one must consider how carbon cycles through various components (vegetation, soil, water and microorganisms) of an ecosystem. Since carbon, in its many forms, is a fundamental element and building block for growth in both plants and animals, it cycles in various ways through living matter. Figure 1.2 illustrates the various pathways of CO_2 in a tundra environments. Essentially, the only pathway through which CO_2 enters the system is via photosynthesis. There are, however, many sources of CO_2. It should be noted that in some environments, there could be a substantial lateral movement of carbon via groundwater flow. However, this pathway is not considered in this study due to the relatively flat topography of the landscape.

1.3.1 Vegetation

CO_2 moves through a vegetated surface via a number of pathways. Plants take in CO_2 through the process of photosynthesis whereby CO_2 and water are converted to carbohydrates with a concomitant release of O_2.

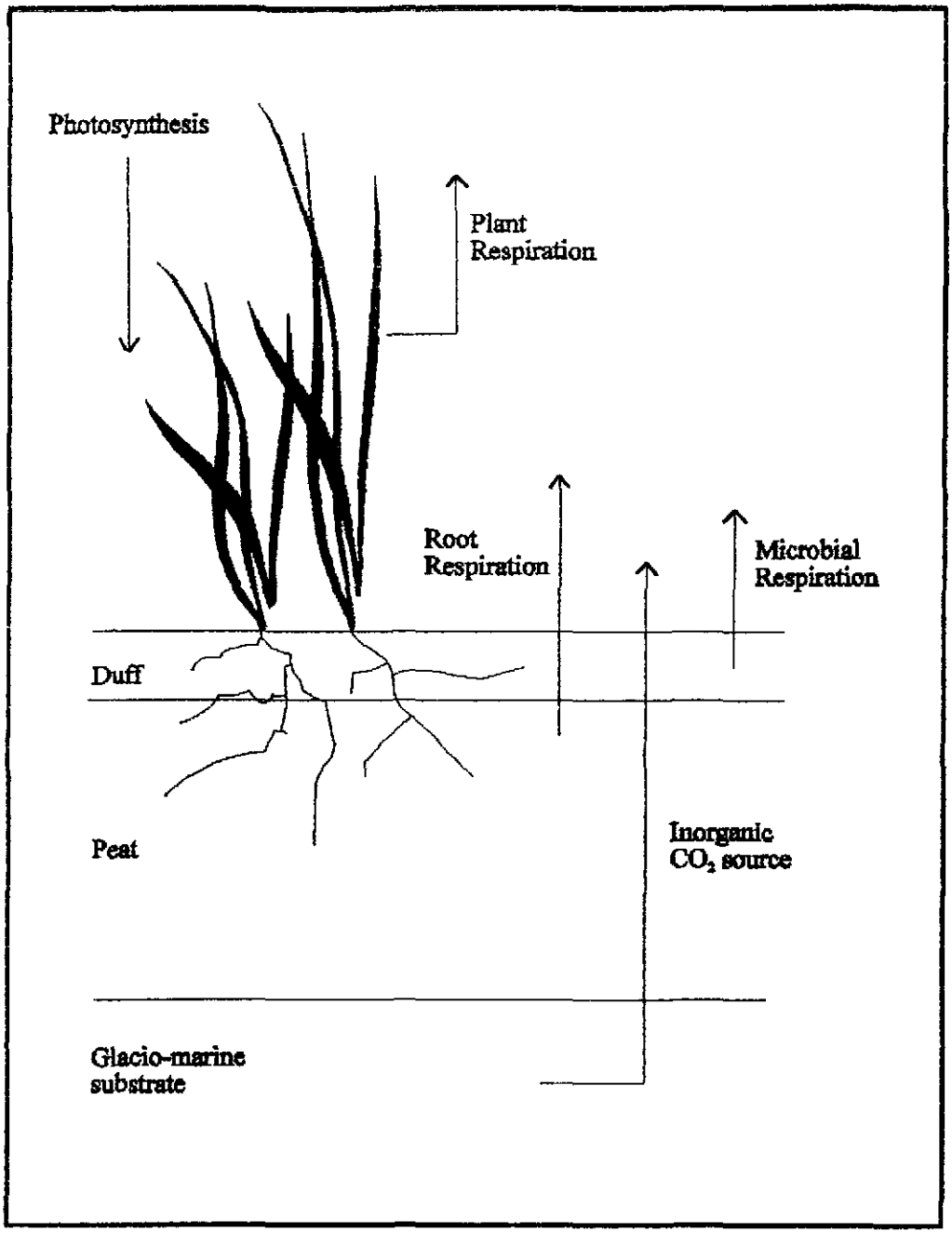

Figure 1.2: Schematic illustration of CO_2 pathways in a tundra environment.

$$6CO_2 + 6H_2O \xrightarrow[chlorophyll]{48\ h\nu} C_6H_{12}O_6 + 6O_2 \qquad (1.1)$$

The formation of 1 mole of sugar, for use by the plant requires the absorption and utilization of 48 photons of radiant energy from the sun. This energy is absorbed by photosynthetic pigments (chlorophyll) in the leaves of plants. This pathway represents a large sink for CO_2 especially in ecosystems where the vegetation canopy is substantial and where photosynthesis is not limited by irradiance, temperature or moisture conditions.

Plants also respire CO_2 during the night (dark respiration) and during the day (photorespiration).

$$C_6H_{12}O_6 + 6O_2 \rightarrow 6CO_2 + 6H_2O + energy \qquad (1.2)$$

Plant dark respiration has two functions. First, it provides the energy required for various biological and chemical processes in the plant and secondly, it provides carbon skeletons that become the basis of other organic compounds (Rosenberg *et al.*, 1983). Photorespiration is a metabolic process that takes place in the chloroplast-containing plant cells, that like respiration, takes up O_2 and releases CO_2 in the light, but which contrary to respiration, ceases in the dark (Larcher, 1980).

In photosynthesis, the chloroplasts use CO_2 of which a supply must be maintained, and liberate O_2. In parallel, both day and night, the cells take up O_2 for respiration and give off CO_2. In assimilating leaves, one or the other of these two opposed processes can dominate

at a given time. The respiration occurring in the light is comprised of both photorespiration and mitochondrial respiration while the processes participating in the dark are mitochondrial and dark respiration.

1.3.2. Soil

In the soil environment, contributions to the CO_2 flux are mainly from respiration of soil organisms and from root respiration (Kim *et al.*, 1992). Peterson and Billings, (1975) and Norman et al., (1992) also note that CO_2 displaced from pore space by water and the release of dissolved CO_2 from warming water may also be sources. Some CO_2 may be produced chemically by the combination of acid rain with limestone soils (Norman *et al.*, 1992).

Microorganisms are continually breaking down organic matter. It is through this process that carbon is broken down and CO_2 is released. This process represents a large source of atmospheric CO_2 especially under conducive temperature and moisture conditions. Where vegetation is sparse, this pathway of CO_2 would dominate.

Root respiration supports growth and maintenance in roots and active uptake of nutrients from the soil solution (Amthor, 1994). It also supports nutrient assimilation (Pate and Layzell, 1990) and is dependent on plant vitality (Mogensen, 1977). In some areas, the proportion of soil CO_2 evolution stemming from root respiration can be quite large. Grammerer (1989) reported that the fraction of soil CO_2 flux in grasslands resulting from root

respiration varied from 15 to 70 % depending on many factors.

1.3.3. Net Flux

Different conventions are used for reporting flux data. Climatologists generally regard a flux directed toward the ground as negative and fluxes directed away from the surface as positive. Therefore, for the sake of clarity, this same convention will be applied to the CO_2 fluxes within the ecosystem. When fluxes are toward the surface, they are considered negative ecosystem exchange (CO_2 taken up) and when they are away from the surface, they are considered positive ecosystem exchange (CO_2 released). The net atmospheric flux is a result of the following pathways:

$$\frac{Net}{Flux} = [(PR + MR + DR) + (RR + IO + MI)] - Photosynthesis \qquad (1.3)$$

PR is photorespiration, *MR* is mitochondrial respiration, *DR* is dark respiration, *RR* is root respiration, *IO* is inorganic CO_2 evolved from weathering of substrate and *MI* is microbial respiration. When *Source* > *Sink*, net fluxes are positive and there is a net loss of CO_2 to the atmosphere. When *Source* < *Sink*, net fluxes are negative and there is a net uptake of CO_2 into the system. By day, most vegetated surfaces exhibit net negative fluxes, where more CO_2 is being taken in by the vegetation than is being emitted to the atmosphere. The flux

magnitude is a function of many factors including leaf area, irradiance, temperature and moisture. At night, photosynthesis does not occur, therefore all systems exhibit a net loss of CO_2, the magnitude of which depends on environmental factors. It follows that if more CO_2 is taken up during the day than is given off via nighttime respiration, the daily flux will be negative. In contrast, if more CO_2 is evolved through respiration processes than is taken up by photosynthesis in the daytime period, the daily flux will be positive. These daily fluxes can be compiled to obtain a seasonal flux for a given system. This value would reflect whether the system is losing or gaining CO_2 over a period of time (e.g. the summertime period) and aids in the endeavor to classify the carbon budgets of different regions and under different environmental conditions.

1.4 Role of Wetlands

Wetlands occupy approximately 18% (170×10^6 ha) of the total land surface of Canada and their character varies greatly in response to climatic and physiographic environments (Zoltai and Pollet, 1983). Wetlands are areas where wet soils are prevalent, where the water table lies near or above the mineral soil and which for most of the thawed season, support a hydrophilic vegetation and exhibit pools of open water (less than 2 m deep)(Zoltai *et al.*, 1973). The greatest concentration of wetlands occurs in a broad belt extending from central Labrador, passing south of Hudson Bay and reaching north-west

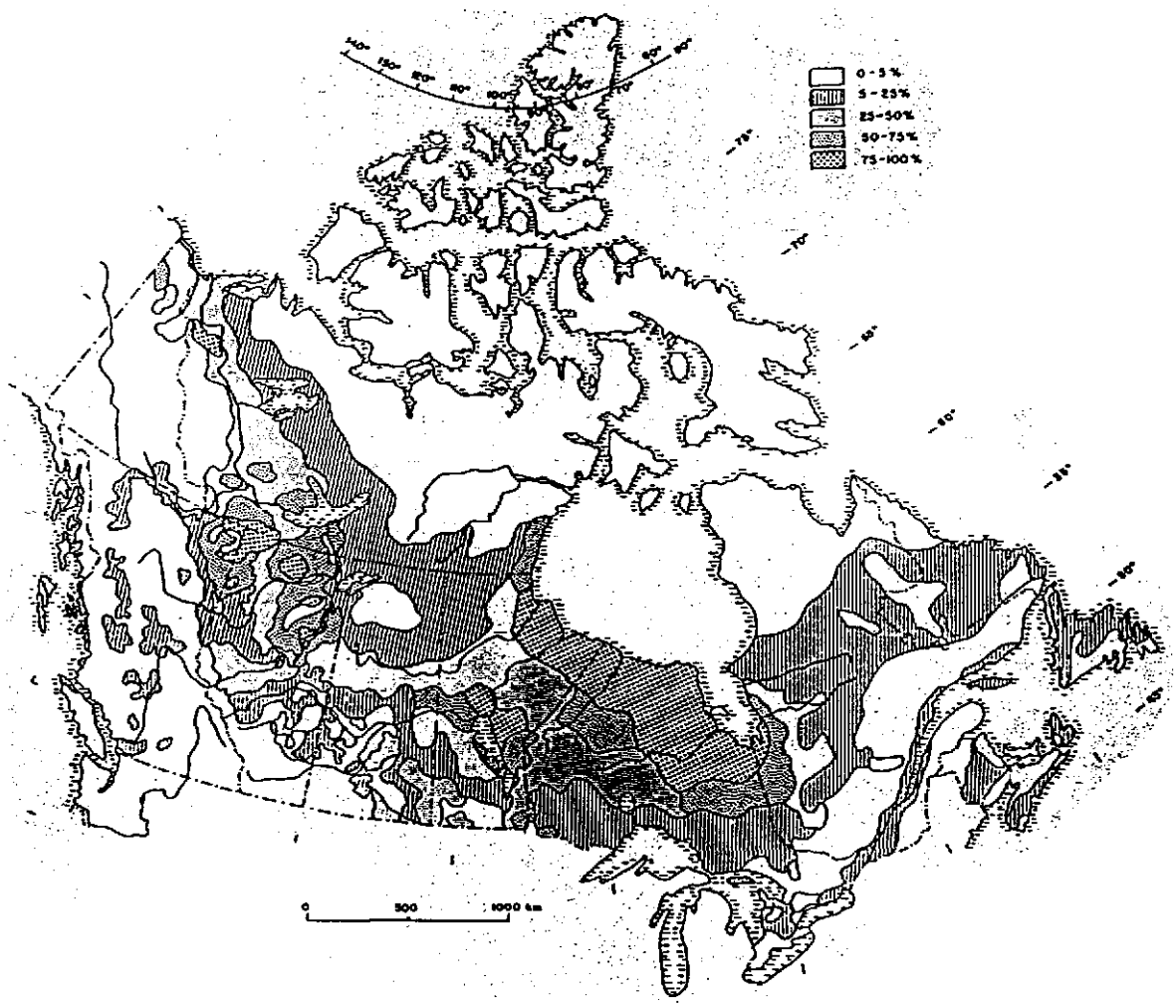

Figure 1.3: Distribution of wetlands in Canada (from Zoltai and Pollet, 1983).

across the northern Prairie Provinces and along the Mackenzie Valley (Figure 1.3). Here precipitation is moderate (400-800 mm annually, decreasing toward the west) and the mean annual temperature is near 0°C, the coolest areas being in the east and north. A cool, moist climate combined with large expanses of flat terrain provide a favourable environmental setting for the development of extensive wetlands. The large area of wetlands west and south of Hudson Bay is the most extensive contiguous wetland in Canada covering some 100 000 km^2 and is classified as a high subarctic wetland region (Zoltai and Pollet, 1983).

These wetlands include peatlands formed by the accumulation of remains of hydrophilic vegetation, but also include areas that are influenced by excess water, but where, for climatic, edaphic or biotic reason, peat is not produced or preserved. Peatlands occupy large areas especially in high latitudes, such as the boreal and subarctic regions of Canada, where 25 to 50% of the land surface may be covered by peatlands totalling approximately 1×10 ha (Tarnocia, 1984; Zoltai and Pollet, 1983). In these regions, low temperatures and low rates of evapotranspiration promote the build-up of slowly decomposing organic matter. Although generally regarded as sinks for atmospheric CO_2, peatlands evolve CO_2 back into the atmosphere through plant respiration and organic matter decomposition (Moore, 1986). Peatlands play an important role in the global cycling of carbon because they store carbon, fixed by plants from atmospheric CO_2, in slowly decomposing organic material (Glenn *et al.*, 1993). Gorham (1991) estimates average historical rates of C accumulation in northern peatlands at 27 g C m^{-2} yr^{-1} and a storage rate of 76 to 96 × 10^{12} g C yr^{-1} for peatlands of boreal and subarctic region. Armentano and Menges (1986) estimate a mean accumulation

rate for temperate peatlands of 48 g C m^{-2} yr^{-1} and an areal storage rate between 57 and 83 $\times 10^{12}$ g C yr^{-1}.

Because of the potential effects of the release of this stored carbon on global climate, the rates and controls on the accumulation and release of carbon in tundra regions are of considerable interest (Miller, 1981; Billings, 1987). There is still controversy regarding whether arctic peatlands are currently a source or sink of CO_2 (Billings, 1987).

With doubling of CO_2 and resulting increases in temperature, Emanuel *et al.* (1985) predict a 37% decrease in the areal extent of the circumboreal subarctic and a 32% decrease in the area of the arctic tundra. Because of these anticipated increases in CO_2 and the possible effects on vegetation, soils, weather and climate, much scientific effort is necessary to quantify these effects on the biosphere (*from* Billings, 1987). Peterson *et al.* (1984) note that concern over increasing levels of atmospheric CO_2 and recognition that peat in northern ecosystems constitutes a large and potentially unstable reserve of world carbon, ultimately necessitates investigating questions concerning the factors that influence net ecosystem exchange in arctic tundra and subarctic ecosystems. Because of their large areal extent and sensitivity to climatic change, northern regions represent a vitally important proportion of the world carbon budget and are thus important in understanding the global response to climate change.

The processes of photosynthesis and respiration in plant and microbial communities exert important controls on the global budget of CO_2 itself and on the cycles of other important nutrients, trace gases, and on water. Quantifying terrestrial biosphere/atmospheric carbon dioxide exchange is critical to understanding global biogeochemical cycles and climate

feedback mechanisms. There is plenty of information on above-ground carbon fixation, but little is known of sensitivity of ecosystem CO_2 efflux to environmental factors (Peterson and Billings, 1975; Luken and Billings, 1985). What is known is limited to coastal tundra areas and bogs.

1.5 Environmental Controls on CO_2 Exchange

An understanding of the mechanisms through which environmental factors affect the carbon balance is essential in predicting the effects of climate change on net CO_2 storage or release by tundra. The most recognized environmental controls on CO_2 exchange are vegetative growth cycles, temperature and water table depth. While in this study, only net fluxes of CO_2 are measured directly, these fluxes are the result of the magnitudes of the various pathways. It is therefore important to understand how each of these processes responds to different environmental conditions in order to accurately interpret the net fluxes.

1.5.1 Temperature

Temperature affects metabolic processes by way of its influence on the reaction kinetics of chemical events and on the effectiveness of the various enzymes involved. In general, Van't Hoff's *reaction-rate/temperature rule* holds, according to which, the reaction rate (k) rises exponentially with temperature. The increase in reaction rate that results from

a temperature increase of 10°C is expressed by the temperature coefficient Q_{10} whereby:

$$\ln Q_{10} = \frac{10}{T_2 - T_1} \ln \frac{k_2}{k_1} \qquad (1.5)$$

T_1 and T_2 are absolute temperatures and k_1 and k_2 are the associated reaction rates. For vegetation, this value is fairly constant over a small range of temperatures and varies between 1.4 to 2.0 for most enzyme reactions and 1.0 to 1.3 for physical processes.

Photosynthesis

Temperature affects photosynthesis through the fixation and reduction of CO_2. The rate of these processes increases as temperature rises until a maximum value is reached, beyond which the rate is maintained over a broad range of temperatures. Not until temperatures are very high, does photosynthesis rapidly decrease.

Dark Respiration and Photorespiration

As temperature rises, dark respiration increases exponentially. Below 5°C, the energy required to activate various processes involved in respiration is large and the Q_{10} factor is high. Above 25 to 30°C, the temperature coefficient for respiration in most plants falls to 1.5 or less. Above this, biochemical processes occur so rapidly that the supply of substrate and metabolites cannot keep pace with the turnover of matter and energy.

Few studies have been done on the relationship between temperature and

photorespiration. However, in principle, it is expected that photorespiration, which relies directly upon photosynthesis for provision of chemical substrate, depends on temperature in the same way as photosynthesis.

Soil Respiration

Temperature directly affects soil respiration by influencing microbial activity. This relationship is also described by the Q_{10} factor. A range of Q_{10} values of 2 to 5 has been reported for various peatland ecosystems (Flanagan and Veum, 1974; Svensson, 1980).

Because CO_2 efflux from the soil is presumably an enzymatic process, the response to temperature is expected to exhibit an Arrhenius-type exponential curve. Evidence for this varies. Peterson and Billings (1975) report a linear daily response of increasing respiration rates with increasing temperature but an exponential seasonal response. Luken and Billings (1985) found similar correlation coefficients using both linear and non-linear methods. Moore (1986) found significant correlations using linear and polynomial regressions. Oberbauer *et al.* (1991) found an exponential response. Kim and Verma (1992) show a linear trend in daily CO_2 flux and peat temperature as do Neumann *et al.* (1994) for midday and nighttime fluxes with bog temperature and air temperature. It has been suggested (Peterson and Billings, 1975) that because CO_2 efflux is the combination of the respiratory activities of different root and microbial populations, that the seasonal response of respiration to temperature may not be exponential.

Many studies of CO_2 evolution from soil have revealed the importance of temperature, especially when dealing with laboratory studies when environmental factors are controlled (e.g. Peterson and Billings, 1975; Billings *et al.*, 1977; Svensson, 1980). It is much more difficult to obtain clear results from field data where the role of many environmental factors cannot be separated. There also seems to be a large degree of variability in the literature about which temperature should affect CO_2 effluxes the most. Some data (e.g. Oechel, *et al.*, 1991) suggests that microbial respiration is a large portion of total soil CO_2 flux, and that microbial populations are concentrated in the upper 10 cm of the soil. It follows that most of the CO_2 evolved would originate from this layer and should be strongly related to temperatures within these layers. The whole soil profile can produce CO_2, but the thermal regime and the greater CO_2 production rates of the surface layers in laboratory incubations suggest that most of the CO_2 emitted is produced in the upper soil layers (Stewart and Wheatley, 1990). Results from Moore (1986) for subarctic peatlands show strong relationships for temperatures closest to the surface, temperature at 5 cm and mean daily air temperature. However, this author suggests that weak relationships may be due to:

1) the release of stored carbon dioxide from subsurface layers of peat as it thaws (Coyne and Kelly, 1974)

2) the depletion of readily available photosynthate

3) the acclimation and reduced late summer growth of plants

4) the variation in nutrient supply

5) the aeration and exhaustion of readily decomposable substrates by mid-summer

6) the production of CH_4 by the decomposition of peat which becomes converted to CO_2 at the peat surface.

Oberbauer *et al.* (1992) found the highest correlations for diurnal CO_2 efflux with temperature at 1 cm depth for riparian tundra communities in the northern foothills of the Brooks Range, Alaska. However, temperatures near the soil surface can change rapidly depending on radiation and wind conditions and therefore a deeper soil temperature, more indicative of average soil conditions, might be expected to provide a better correlation. For example, Oberbauer *et al.* (1991) found that temperature at 5 cm provided a better overall correlation with CO_2 efflux in drier tussock and water track tundra than did temperature at 2 cm. Soil water content may account for these differences since high soil water contents tend to buffer rapid changes in surface temperatures.

To minimize the confounding effect of water table, Kim and Verma (1992) plotted daily soil CO_2 fluxes against peat temperature at 10 cm for different ranges of water table depth. The rate of CO_2 evolution was temperature-dependent and this dependence was stronger when water depths were greater.

1.5.2 Water Table and Soil Moisture

The level of the water table defines the size of the aerobic zone in the soil profile thus the degree to which microbial activity can contribute to soil CO_2 evolution. Also, soil moisture status influences the health of vegetation, thereby influencing the CO_2 uptake by

photosynthesis.

Small variations in the water table affect CO_2 exchange to a greater extent than moderate changes in other environmental factors such as temperature (Billings *et al.*, 1982), atmospheric CO_2 concentrations (Billings *et al.*, 1983) and to a greater extent than microsite variability (Billings *et al.*, 1982). Previous studies by Peterson *et al.* (1984) indicated that significant reductions in carbon storage or increases in net carbon release from Arctic tundra are initiated by recession of the water table by as little as 5 to 10 cm. These authors hypothesized that reduced carbon uptake or increased carbon loss by microcosms under conditions of a lowered water table could be explained by:

1) a lower incorporation of carbon by plants through decreased photosynthetic rate or increased respiratory losses of living plant tissue above or below the ground; or

2) increased microbial release of soil carbon as CO_2 flux from the soil surface.

Photosynthesis

Water is used in photosynthesis, but it is not in this sense that water is a limiting factor. More important is that water is necessary to maintain a high water potential in the protoplasm, therefore the metabolic processes of the cell are critically dependent upon water. Loss of water has a direct inhibitory effect on this photosynthetic process. The main result of loss of turgor is closure of the stomata, which results in an interruption of the CO_2 supply. In addition, respiration and photorespiration in particular, are reduced during water deficiency.

Thallophytes

Thallophytes draw water by capillary action from damp substrates and from their surfaces after wetting by rain, dew and fog. When saturated with water, lichens and peat moss can contain up to 15 times as much water as in the dry state (Larcher, 1980). Most mosses can contain 3 to 7 times the amount of water when saturated than in their dry state, while lichens can contain 2 to 3 times as much. Thallophytes, although they soak water up rapidly, also lose water rapidly through evaporation. Therefore their water contents may vary rapidly over short periods of time. An ecologically important measure is the humidity compensation point. The minimum atmospheric humidity for net photosynthesis to occur is ~80 to 96% for lichens and ~90% for mosses. As more water is taken in, the rate of photosynthesis rises rapidly, becoming maximal in the optimum turgor range. In lichens, this occurs between 50 and 80% of the water content at saturation. CO_2 uptake declines when the plants are full of water. During desiccation, photosynthetic activity gradually diminishes and respiration is suppressed. The photosynthetic apparatus of thallophytes is well-suited to the frequent and pronounced fluctuation in the cellular water content. Completely dry thalli reactivate the photosynthetic process within minutes after they receive water again, even if they have been dried out for a long period of time.

Vascular Vegetation

Water affects vascular vegetation through the activity of the stomates. The stomatal openings will become narrow during water stress, the result of which slows down CO_2

exchange. Normally, CO_2 uptake is high only over a narrow range of the adequate water supply level, beyond which it declines and eventually is entirely suspended.

There are therefore two critical points in the curve of CO_2 exchange versus water loss. The first is the point of transition from full capacity to the limited region and the second is the null point for gas exchange. The first point comes at a level of water stress in which the stomata begin to close, causing the stomatal diffusion resistance to increase. If water is supplied after this, recovery can be rapid. The second critical point is determined by marked or complete closing of the stomata as well as by the direct effect of water shortage on the protoplasm. Appreciable CO_2 uptake is no longer possible, though the CO_2 freed by respiration can be bound again. Once this state has been reached, a renewed water supply does not lead to an immediate recovery of photosynthesis. Recovery is delayed and after severe desiccation, the original photosynthetic capacity may, under certain conditions, never be achieved again.

The variable response of vegetation to changes in water table position or soil moisture may also be explained by considering different rooting systems. For example, Peterson *et al.* (1984) note that the much-branched roots of *Dupontia* are near the soil surface and within the zone of water table fluctuation. The roots of *Carex* plants are much thicker, less branched and penetrate more deeply into the soil (e.g. Billings et al., 1978). Therefore, species of *Dupontia* would be exposed to fluctuating soil moisture conditions, while *Carex* species would be relatively unaffected because their roots extend farther and can tap moisture at greater depths.

Soil Respiration

Controlled laboratory studies using soil columns have identified the influence of water table position on CO_2 flux. Moore and Knowles (1989) found for swamp microcosms that lowering of the water table increased CO_2 flux in an approximate linear manner. The flux when the water table was at a depth of 70 cm beneath the peat surface was 9 times that when the water table was at the peat surface. Billings *et al.* (1983) using tundra microcosms from Barrow, Alaska estimated an annual net gain of 119 g CO_2 m^{-2} when the water table was at the surface compared to an annual net loss of 476 g CO_2 m^{-2} when the water table was just 10 cm below the surface.

There are few field studies which report significant relationships between water table position and CO_2 efflux because other environmental variables cannot be controlled. Kim and Verma (1992) found it difficult to discern any distinct relationship between water table depth and CO_2 efflux at low to moderate temperatures at 10 cm within the peat profile ($5<T<15$°C). However, the soil flux was almost linearly related to water table position when temperature exceeded 15°C.

CHAPTER 2

CO_2 Flux Calculation

The Gradient Theory

The raw CO_2 flux can be calculated as:

$$F_c = -K_c \cdot \frac{\partial \overline{\rho_c}}{\partial z} \tag{2.1}$$

where K_c is the turbulent transfer coefficient and $\partial \overline{\rho_c} / \partial_z$ is the mean CO_2 density gradient. From the measured sensible heat (Q_H) using the BREB approach (see Appendix B), and by assuming the similarity of transfer coefficients, K_c is then equivalent to:

$$K_c = K_h = \frac{-Q_H}{(\partial T/\partial z)\ c_p\ \overline{\rho_a}} \tag{2.2}$$

where $(\partial T/\partial z)$ is the temperature gradient, c_p is the specific heat of dry air and $\overline{\rho_a}$ is the density of dry air. Transforming $\partial \overline{\rho_c} / \partial_z$ into finite difference and making use of the measured CO_2

concentration gradient, $(\Delta\overline{C}/\Delta z)$ in ppmv m^{-1} (equivalent to µmol mol^{-1}) gives:

$$\frac{\Delta\overline{\rho}_c}{\Delta z} = \overline{\rho}_a\left(\frac{m_c}{m_a}\right)\left(\frac{\Delta\overline{C}}{\Delta z}\right)\cdot\left(10^{-6}\frac{mol}{\mu mol}\right) \qquad (2.3)$$

where (m_c/m_a) is the ratio of molecular weight of CO_2 to the molecular weight of air. Upon applying this conversion,

$$F_c - raw = -\left(\frac{-Q_H}{(\Delta T/\Delta z)\,c_p}\right)\left(\frac{m_c}{m_a}\right)\left(\frac{\Delta\overline{C}}{\Delta z}\right)\cdot\left(10^{-6}\frac{mol}{\mu mol}\right) \qquad (2.4)$$

Simplifying and collecting the constants into the following term,

$$\lambda = \left(\frac{m_c}{m_a}\right)\left(\frac{10^{-6}}{c_p}\right) \qquad (2.5)$$

reduces the equation for F_c to:

$$F_c - raw = \lambda\left(\frac{Q_H}{\Delta T/\Delta z}\right)\cdot\left(\frac{\Delta\overline{C}}{\Delta z}\right) \qquad (2.6)$$

in mg m^{-2} s^{-1}. The BREB method can become problematic when Q^* is small and thus subject to errors in Q_G measurements. In this situation, the partitioning of energy between Q_H and Q_E is affected and recognized by the different flux directions of Q_E and Q_H between the BREB

and aerodynamic flux calculation methods. In this case, the aerodynamic method (see Appendix B) is used in place of the BREB method. The aerodynamic approach to the calculation of Fc - raw from profiles of the mean concentration gradient and wind speed is given by the following equation where:

$$F_c - raw = -\left[k \cdot \overline{\rho_a}\left(\frac{m_c}{m_a}\right)\left(\frac{\partial \overline{C}}{\partial \ln z}\right)\cdot 10^{-6} \cdot \mu^*\right](\phi_m \phi_c)^{-1} \qquad (2.7)$$

k is von Karmon's constant (0.4), ϕ_m and ϕ_c are the dimensionless stability corrections for momentum and CO_2 respectively and μ^* is the friction velocity expressed as:

$$\mu^* = k\left(\frac{\partial \overline{\mu}}{\partial \ln z}\right) \qquad (2.8)$$

Equation 2.7 was multiplied by 10^6 to convert the fluxes into mg m^{-2} s^{-1}.

The Webb correction (Webb *et al.*, 1980) was then applied to account for density changes due to the flux of heat and water vapour. It is given by the following equation:

$$F_c = F_c - raw + \left[\frac{\overline{\rho_c}}{\overline{\rho_a}}\left(\frac{\mu}{1 + \mu\sigma}\right)\frac{Q_E}{L_v} + \frac{\overline{\rho_c}}{\overline{\rho}}\left(\frac{Q_H}{c_p \cdot \overline{T}}\right)\right] \cdot 10^6 \qquad (2.9)$$

where F_c is the CO_2 flux in mg m^{-2} s^{-1}, Q_E is the latent heat flux in W m^{-2}, L_v is the latent heat of vaporization, $\overline{\rho}$ is the total density of the air ($\rho_a + \rho_v + \rho_c$) and $\overline{T}$ is the mean air

temperature in °K. Quantities μ and σ are given as:

$$\mu = \frac{m_a}{m_v} \tag{2.10}$$

$$\sigma = \frac{\overline{\rho_v}}{\overline{\rho_a}} \tag{2.11}$$

where m_v and $\overline{\rho_v}$ are the molecular weight and mean density of water vapour respectively.

The first part of the square brackets in Equation 2.9 is the correction factor for water vapour and the second part is the correction for sensible heat. The first correction may be omitted if air samples are desiccated and maintained at a constant pressure. The sensible heat correction may be omitted if the air samples are brought to a common temperature and pressure before entering the gas analyzer. The heat correction could be omitted from this equation since the analyzer was insulated (see Chapter 3, Section 3.2.4) and sample temperatures were found to be within 0.1 °C of each other.

CHAPTER 3

Site Description and Methodology

3.1 Site Description

The research area is located along the north-west coast of Hudson Bay, within the Hudson Bay Lowland. It lies within the southern limit of continuous permafrost and at the northern extent of the northern boreal treeline (Figure 3.1, insert). The site itself, is located approximately 20 km east of the town of Churchill, Manitoba (58°45'N, 94°04'W) and approximately 12.5 km south of the Hudson Bay coastline (Figure 3.1).

The site is an extensive fen which means that it has restricted drainage, low oxygen saturation, and a restricted mineral supply and is characterized by typical hummock and hollow surface relief. The hummock height averages about 0.25 m above the ground surface, but ranges from 0.12 to 0.50 m. A survey was conducted to determine spatial coverage of hummocks, hollows and ponded water at the site. Surface coverage was recorded at 1 m intervals for 20 m along transects oriented in north, south, east and west directions. The surface coverage on June 13 was hummock (38 %), hollow (52 %) and ponded water (10 %). By June 17, ponded water had disappeared from the site and the surface coverage changed to hummock (38 %) and hollow (62 %) and remained

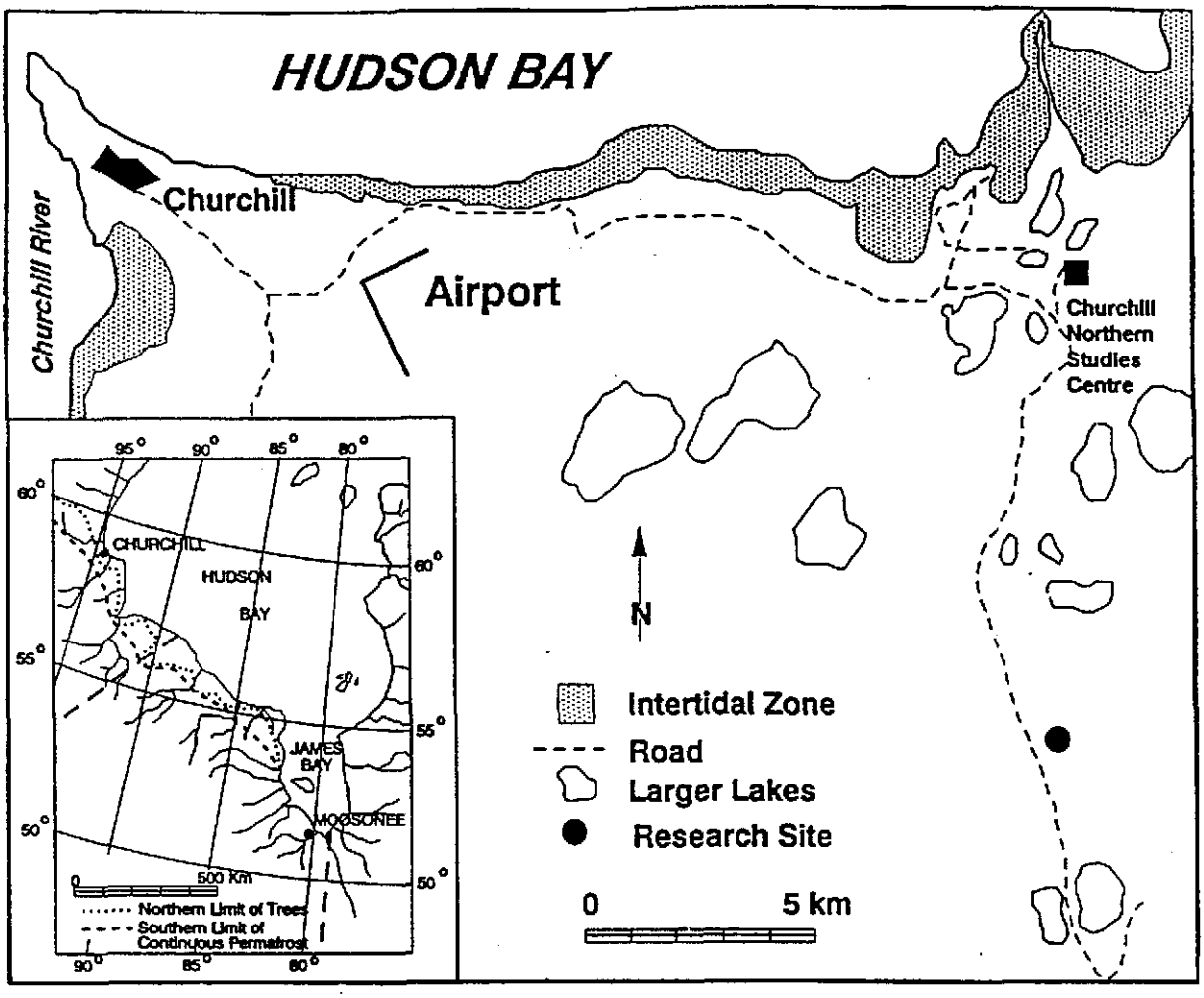

Figure 3.1: Location of the study site.

unchanged throughout the remainder of the season.

The base of the soil profile is glacio-marine till, comprised of fine silts and clays and containing layers of carbonate shingles. Above this is a more recent accumulation of peat (partially decomposed organic matter) which is approximately 0.20 to 0.30 m thick at this site. Given estimates of isostatic rebound of 1 m per century for this region, it is only 2000 years since emergence from the Tyrell Sea. Peat accumulation rates have been estimated at 1 mm yr^{-1} for coastal regions, and 2 mm yr^{-1} for inland areas (Burton *et al.*, 1995). Overlying the profile is a surficial porous layer of partially decomposed organic matter and mosses, commonly referred to as '*duff*'.

The vegetation is dominated by sedge species (*Carex aquatilis, Carex saxatilis, Carex gynocrates*) and is sparsely populated with a vascular shrub canopy including species of *Betula glandulosa, Ledum decumbens* and *Salix arctophila*. The ground surface is entirely covered with moss (*Scorpidium turgescens*) and to a lesser extent, various lichen species, such as *Cladina stellaris* and *Cladina rangiferina*. The growth period began before June 6, with maximum growth occurring during the fourth week of July. The maximum leaf area of 0.29 m^2 m^{-2} for sedge species was reached on July 13. The maximum shoot density was 1008 shoots m^{-2} on July 28 and the maximum canopy height of 17.7 cm was reached on July 27. The senescence of vegetation began the first week of August.

3.2 Methodology

3.2.1. Environmental

Air Temperature and Vapour Pressure

Temperature and vapour pressure profiles were measured using wet- and dry-bulb psychrometry. Housings were mounted at 0.35, 0.70, 1.1, 1.6, 2.3 and 3.2 m on a meteorological tower (Figure 3.2). The styrofoam housings were covered with reflective tape to reduce heating and aspirated with fans generating an air flow of ~5 m s^{-1} which were powered by a series of 12V marine batteries. Within the housings, wet- and dry-bulb temperatures were measured with copper-constantan thermocouples encased in stainless steel tubing. The wet-bulb was covered with a cotton sheath which continually wicked water from a distilled water reservoir next to the housing. These reservoirs were checked and filled periodically with distilled water and the wet-bulbs were checked regularly for dry wicks. Each wet-bulb thermocouple was referenced to the corresponding dry-bulb thermocouple positioned at the same height. Each dry-bulb thermocouple was then referenced to a ground temperature plug which was referenced to the datalogger panel temperature. This was necessary to eliminate any temperature differences across the input cards in the datalogger (Halliwell, 1989).

Wind Speed and Direction

Wind speed was measured using six 3-cup anemometers (Young, Model 12102,

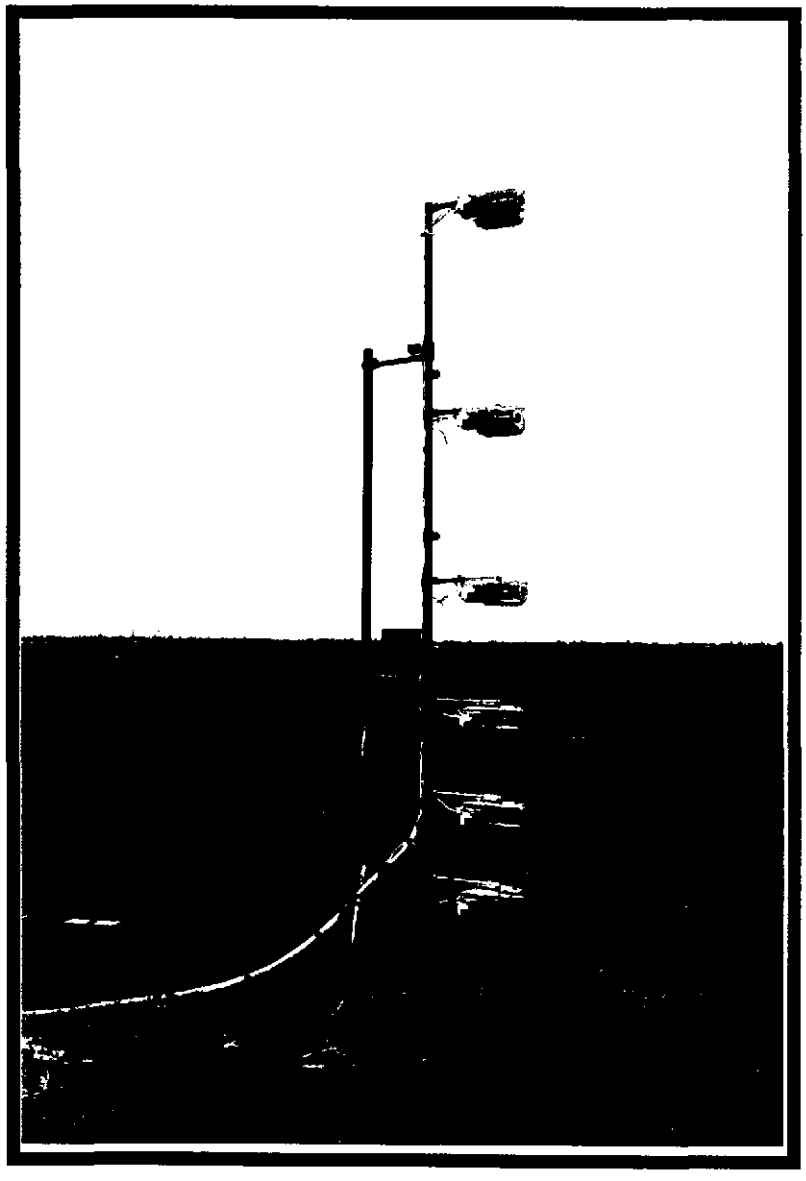

FIGURE 3.2: Meteorological tower with temperature and vapour pressure instrumentation.

FIGURE 3.3: Meteorological tower with wind speed, wind direction and net radiation instrumentation.

Traverse City, Michigan, U.S.A.) mounted facing west on a separate meteorological tower at the same heights as the psychrometers (Figure 3.3). Wind direction was monitored using a wind vane (Young, Model 05103) mounted on top of the tower, approximately 3.5 m above the ground surface.

Precipitation and Water Table

Precipitation was measured using both a standard rain gauge and a tipping bucket rain gauge (Weathertronics, 6010). The daily water table position was measured with respect to a reference level above the surface in a well constructed from perforated ABS plastic pipe (5 cm diameter). This was done manually using a meter stick equipped with a water sensitive electronic beeper. Continuous fluctuations in the water table level were monitored by suspending a float and counterweight to a pulley which was attached to a potentiometer. Fluctuations in the water level affected the voltage output and these signals were converted to a water level by a datalogger.

Active Layer Depth

The position of the frost table below the ground surface was measured regularly using a thin metal probe approximately 1.5 m in length. The probe was inserted into the ground surface until contact was made with the frost table or until further movement was impeded. Multiple readings were taken because in some instances the probe was actually hitting rock or a carbonate shingle layer that is present at ~0.30 m in the soil profile. Since the frost table

level is quite variable spatially, especially in hummock/hollow terrain, 6 measurements were made in selected hollows, and 6 were made in selected hummocks. The same point of entry was not reused when probing, because water and heat could preferentially flow down these conduits, therefore enhancing melt at greater depths.

The progression of the frost table could also be generated by recording the depths of 0°C isotherms within the soil profile. This method is compared with manual measurements.

Soil Moisture

Volumetric soil moisture was measured on 7 occasions throughout the study period. A block of soil (~0.30 m × 0.30 m × 0.30 m) was dug out of the ground to facilitate sampling. A 125 cm^3 steel soil tin was placed on the soil face and the perimeter of the sample was cut with a sharp knife. The tin was then gently pushed in circular fashion into the soil. This was done to avoid compressing the sample and therefore overestimating its bulk density and also underestimating the water content. A knife was also used to cut into the soil across the opening of the can before it was pulled out. This procedure minimized impact on the soil core to ensure accuracy. Samples were taken at the soil surface (~10 cm below the duff) and at ~20 cm below the soil surface. To achieve a representative value, hummock and hollow areas were sampled. Upon completion, samples were weighed in the lab on a digital scale (Ohaus, CT Series, model 65081) with a resolution of 0.1 g and a precision of ±0.1 g. The samples were then put into a drying oven at 100°C for 24 hours and then reweighed. The volumetric soil moisture (θ_v) was calculated as:

$$\theta_V \quad \frac{W_W \quad W_D}{V_c} \times 100\% \qquad (3.1)$$

where W_W is the wet weight of the sample (including the can), W_D is the dry weight (including the can) and V_c is the volume of the sampling can.

3.2.2 Vegetation

Five random plots were selected by tossing a 25 cm^2 grid within a controlled area. Within each plot, all the above-ground sedge species were harvested and collected. A random selection was chosen to achieve a representative sample of leaf area from both hummock and hollow surfaces. In the laboratory, dead matter was removed from the samples which were then left to air dry in paper bags. Once back at McMaster University, all samples were weighed on a balance (Oertling, Fisher Scientific, Model R20, Serial No. 19141A). To achieve the area of the whole sample, a known weight:area ratio was applied to the weights of these samples. This ratio was obtained in the field by collecting large leaves of similar species (n=32), calculating the surface area and obtaining the dry weight. The ratio was 1 g dry weight : 258 cm^2.

Shoot density was measured on 5 randomly selected 25 cm^2 plots on 7 days throughout the summertime period. Within each plot, the number of living sedge shoots (whole plants) was counted. Shoot elongation was measured using a ruler on 50 randomly selected sedge samples on each of 7 days throughout the study period.

Stomatal Conductance

Stomatal conductance of sedge species was measured using a steady-state porometer (LI-1600, Li-Cor, Lincoln, Nebraska, U.S.A.). The theory used for calculating conductance is included in Appendix C. Although this is not a direct measurement of photosynthesis, it is assumed that measurements of stomatal behaviour does reflect patterns of photosynthesis. Measurements were made at hourly intervals on 6 days throughout the month of July and recorded on cassette tape and later downloaded to computer using an interface (C20, Campbell Scientific). Measurements were generally made between 0600 ST and 2000 ST to obtain a diurnal pattern of stomatal behaviour. Sunrise and sunset measurements were not feasible however, due to the possible damage of the fine wire thermocouple from dew. Three healthy sedge samples were used for measurements. If samples became damaged or apparently stressed from measurement, then new samples were selected.

The porometer's small aperture (Serial No. 1600-06) was used. This has dimensions of 4.8 mm × 13.7 mm and covers a total area of 0.60 cm^2. Since most species of sedge are amphistomatus, conductance from both sides of the leaf was measured and later, totalled.

3.2.3 Radiation and Energy

Net Radiation

Net allwave radiation was measured using a pyrradiometer (Middleton, CN-1, Melbourne, Australia) mounted at the height of 2.9 m near the top of a 3.5 m

meteorological tower (Figure 3.3). The pyrradiometer was oriented due south to minimize shadow effects. Polyethylene domes on the instrument were kept inflated with dry air through an aspiration system consisting of a pump which forced air through a tube of indicating silica gel and then into the instrument. The silica gel was changed regularly to ensure the dryness of the air.

Shortwave radiation ($K\uparrow$ and $K\downarrow$) was measured using Eppley black and white pyranometers (Model 8-48, Newport, Rhode Island, U.S.A.). A quantum flux density sensor was used to measure photosynthetically active radiation (PAR) in the 0.4 to 0.7 μm waveband (Licor, Model LI-190SB, Lincoln, Nebraska, U.S.A.).

Ground Temperature and Ground Heat Flux

Ground temperatures at the site were measured in a flat grass area at depths of 0.05, 0.10, 0.20, 0.30, 0.40, 0.50, 0.60, 0.70, 0.80, and 0.90 m using thermocouples inserted into a ground temperature rod. Three supplementary rods measured ground temperatures at 0, 0.05, 0.10, 0.20 and 0.30 m depths at a location close to the study site (approximately 50 m south east of the main tower). These were placed in representative hummock, hollow, and flat areas.

Surface temperatures were measured using four thermocouple arrays. Each array consisted of five thermocouples connected in series to obtain a spatial average. One array was placed in a hummock, one in a hollow and two were placed in ponded water. The water, however, dried up soon after the arrays were installed. To install an array, the center

was inserted into a cut in the top of the peat and each thermocouple wire was implanted radially out from the center. Thermocouples were inserted into the top 5cm of the peat just below the vegetation to reduce heating from direct sunlight. Periodically, thermocouple wires had to be pushed back into the peat since the drying of the surface caused subsidence.

To measure the ground heat flux, four heat flux transducers were inserted approximately 5 cm beneath the soil surface ensuring that the plates were horizontal and that good contact was made between the plate and the peat. Heat flux plates were placed in a hollow, hummock, ponded water and a flat area.

Halliwell and Rouse (1987) found that transducers underestimate ground heat flux by ~50%. The cause of this error is due to poor thermal contact between organic material and the plate. To correct for this underestimation, the calorimetric correction employed by Halliwell and Rouse (1987) was used in this study. This requires a knowledge of soil characteristics at depth, in order to estimate the heat capacities and subsurface temperatures.

3.2.4 Net Ecosystem Carbon Dioxide Fluxes

Sampling intakes were located inside the psychrometers housings (Figure 3.4). Air was drawn down Bev-a-line tubing by a Brailsford 12V DC powered pump into 1L Nalgene buffer volumes. From here, samples were drawn selectively into solenoid-actuated valves on an intake manifold. This manifold acted to split flow into that which was being sampled and the remaining five samples. During sampling, the sampling pump would provide suction

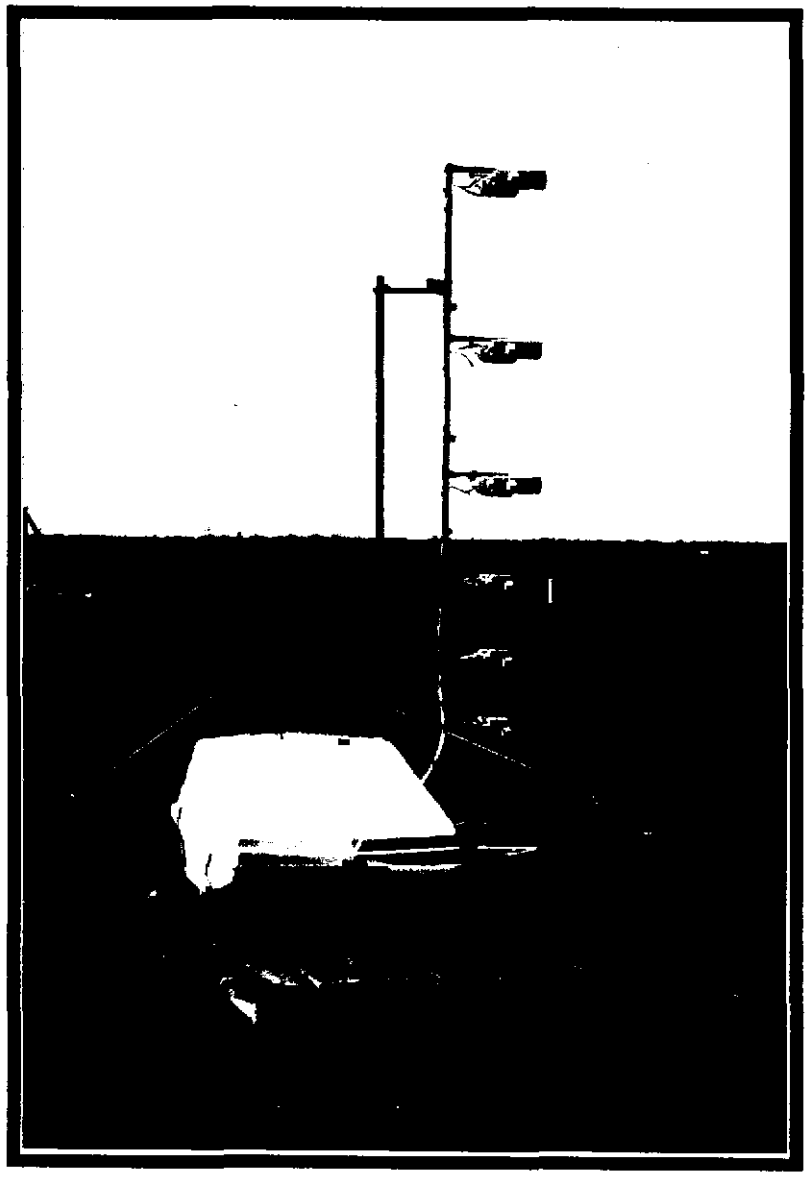

Figure 3.4: The CO_2 field measurement system.

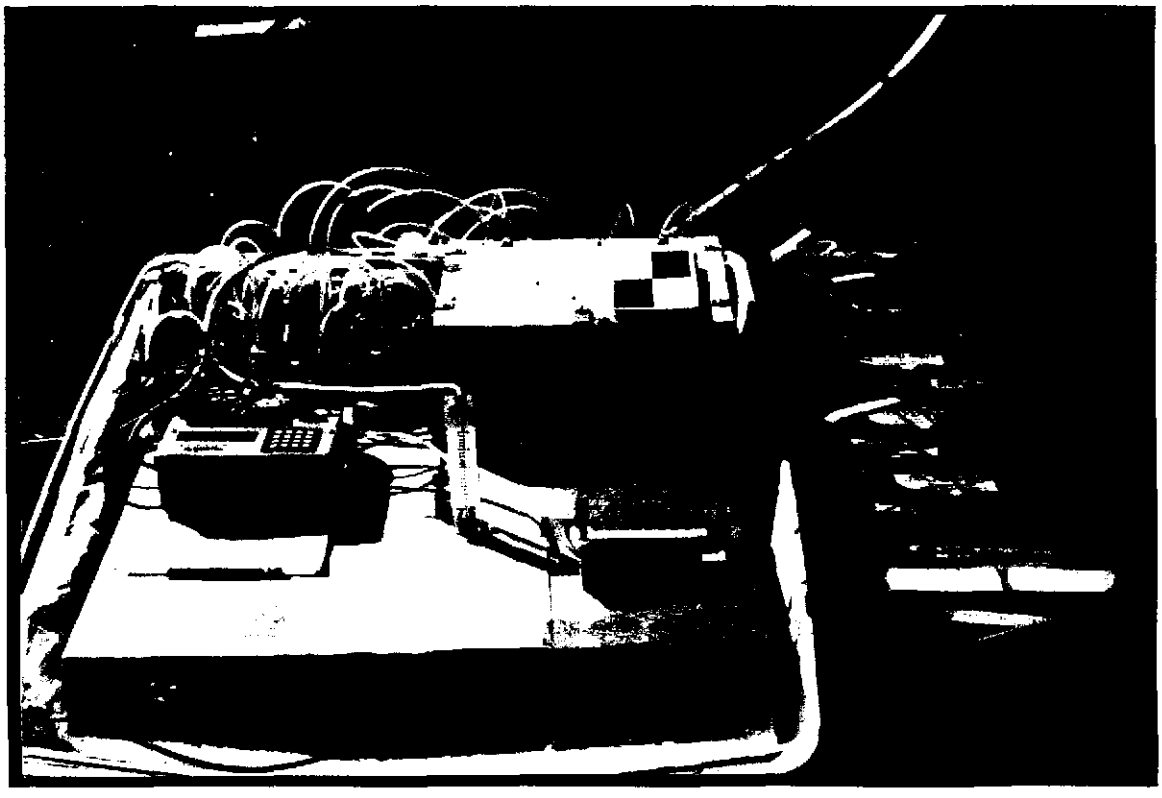

FIGURE 3.5: CO_2 instrumentation housed in the environmental enclosure.

to the valve which was open, while the circulation pump would draw down air from the remaining five levels. The flow of air was maintained between 1.8 to 2.0 L min^{-1} by a flow meter. An amplifier panel was used to generate the 12V required by the solenoid valves because the digital control ports in the 21X only output 5V. LED's (light emitting diodes) on the amplifier panel indicate which level is being sampled, and can be shut off to conserve power.

A 10 second sampling rate was chosen, since it took 7 seconds for the air sample to travel from the intake to the IRGA. Thus, all intake levels were sampled once in a minute. The IRGA (Li-Cor, Model LI-6262) is a non-dispersive, infrared gas analyzer. CO_2 measurements are based on the difference in absorption of infrared radiation passing through two gas sampling cells. The reference cell is used for a gas of known concentration and the sample cell is used for a gas of unknown concentration. Infrared radiation is transmitted through both cell pathways, and the output of the analyzer is proportional to the difference in absorption between the two. In this application, the IRGA was used in absolute mode whereby the reference pathway is continually purged of CO_2 and water, by a scrubber positioned in the reference pathway which contains soda-lime to absorb CO_2 and magnesium perchlorate to absorb water. These chemicals were replaced approximately every 3 weeks. The IRGA was calibrated regularly using a standard gas (344 ppm) and ultra high purity (UHP) nitrogen.

The IRGA was encased in an insulating cabinet in order to increase the sample gas temperature so that it approached the optical bench temperature (~37°C) (Figure 3.5). This

was achieved by utilizing the IRGA's own heat generation. A 1 m length of ¼" copper tubing was coiled in wave form on top of the IRGA. The whole unit was placed within a cabinet which was filled with polystyrene foam. The IRGA heated the copper tubing which, in turn heated the air. This heating system was successful in bringing the sample temperature within 2 to 3°C of the optical bench temperature. This sample gas temperature was measured by inserting fine-wire thermocouples into the Bev-a-line sampling tube before it entered the IRGA, and at the outlet. The sample temperature before and after it entered the IRGA, the optical bench temperature and the cabinet temperature were continually monitored by a Campbell 21X datalogger.

3.3 Data Analysis

The study period extended from June 13 to August 26. The data set was subdivided based on the contribution of vegetation to net ecosystem exchange of CO_2. Observations of the phenological growth stage of the sedge species and the patterns in the daytime net ecosystem exchange over the season clearly illustrated three distinct periods. Period I, which extended from June 13 to June 21, was distinguished by a small presence of vegetation, therefore exhibited no daytime periods for which absolute photosynthesis was dominant. Period II encompassed June 22 through August 8 and represented the period of maximum vegetation growth. During this period, photosynthesis generally dominated net

ecosystem exchange during the day. Period III extends from August 9 to August 26 and is marked by senescing vegetation and absolute photosynthesis dominated daytime fluxes on only two occasions.

CHAPTER 4

Results and Discussion

4.1 Environmental Setting

4.1.1 General Climatic Conditions

The daily average air temperature in June, July and August (J-J-A) was 11.8 °C (Table 4.1), a full 2 °C warmer than the 50-year average (1943-1993). Daily temperatures ranged from 3.2 to 21.0 °C (Figure 4.1). Daytime and nighttime temperatures were similar in Periods I and II, whereas daytime temperatures in Period III were cooler. Surface and soil temperatures were warmest during Period II (Table 4.1).

During J-J-A there was only 71 mm of rain (Figure 4.2a), less than one-half the 50-year average of 156 mm. Period I received 4 mm of rain in 3 events. In Period II, 32 mm of rain fell in 15 rain events while Period III received 36 mm of precipitation in 11 events.

The depth of the 0 °C isotherm indicates that the frost table retreated from -0.24 m at the beginning of measurements to -1.12 m at the end (Figure 4.3). The average rate of thawing was 0.01 m d^{-1}.

Surface moistures ranged from 55 to 72 % by volume (Table 4.2), while subsurface

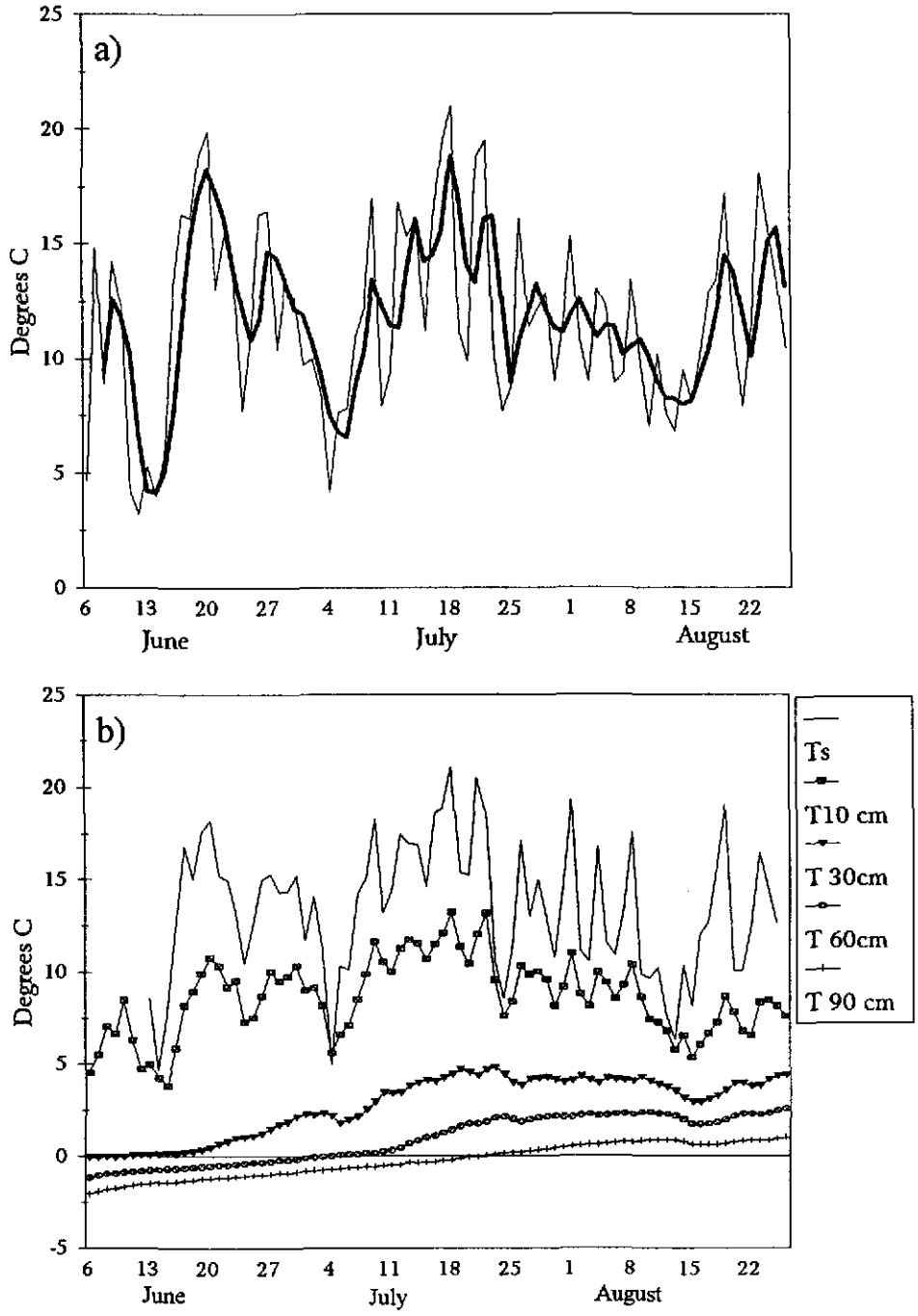

Figure 4.1: a) Daily mean air temperature (thick solid line is the 3-day running mean and b) Seasonal ground temperatures.

Table 4.1: Average air and soil temperature (°C)..

		Seasonal	Period I	Period II	Period III
Tair	**Daily**	11.8	12.5	12.3	11.1
	Day	14.1	14.8	14.5	12.9
	Night	8.7	8.2	8.7	8.8
Ts	**Day**	17.7	16.2	18.8	15.5
	Night	6.9	6.8	7.0	6.7
T @ 5 cm	**Day**	11.2	10.4	12.8	9.4
	Night	8.1	8.4	7.8	7.4
T @ 10 cm	**Day**	8.0	7.4	9.2	6.9
	Night	7.4	7.5	7.6	7.0
T @ 20 cm	**Day**	4.5	3.1	6.3	5.1
	Night	4.2	3.4	5.1	5.3
T @ 30 cm	**Day**	2.3	0.2	4.5	4.1
	Night	1.9	0.3	3.1	4.1

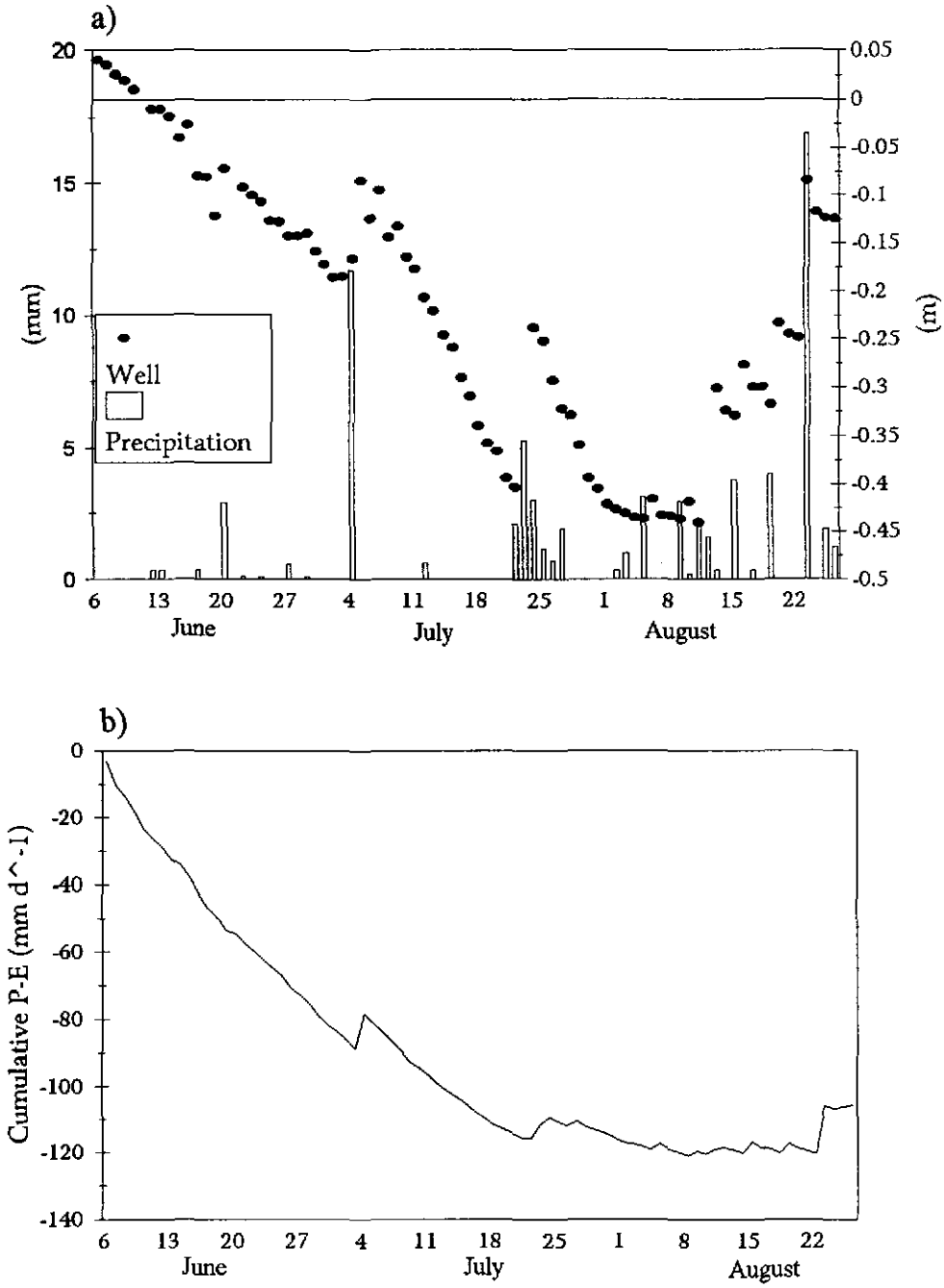

Figure 4.2: a) Seasonal precipitation and water table depth and b) Cumulative water balance.

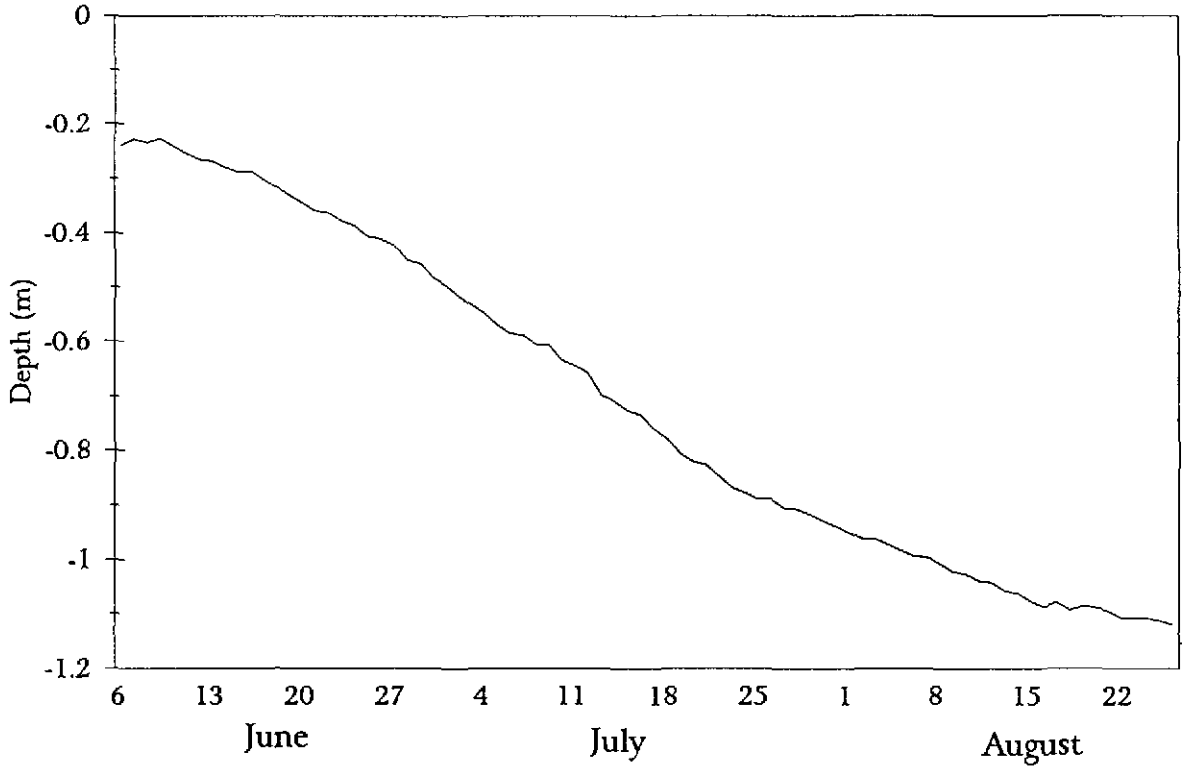

Figure 4.3: Seasonal progression of the frost table.

moistures were larger and ranged from 59 to 77 % by volume.

The average daily windspeed over the entire season (June 6 to August 26) was 3.1 m s^{-1} and ranged from 0.8 to 6.4 m s^{-1}. The dominant wind direction over the entire study period was from the north, followed closely by winds originating in the south-west.

4.1.2 Energy and Water Balance

Table 4.3 indicates the important features of the energy and water balance which are related to the CO_2 budget. Both solar and net radiation and the ground heat flux showed the normal decrease from the long days of the summer solstice (daylength 18h 32') to the last day of measurement in August (daylength 14h 42'). The proportion of net radiation used in warming the ground was consistent throughout the season at 11 to 12%. The largest variability was found in the evaporative and sensible heat fluxes. Q_E declined by almost one-half between Periods I and II and the Bowen ratio (β) more than doubled. Period III witnessed a further decline in the magnitude of Q_E but β decreased slightly.

The water balance (P-E) indicates a large deficit in Periods I and II and a water surplus in Period III. The cumulative seasonal water deficit is shown in Figure 4.2b. The fen experienced a maximum water deficit of approximately 120 mm in Period III, after which recharge began. The average seasonal deficit over the entire season was 106 mm. This is the largest deficit reported for this site in 29 years.

Table 4.2: Mean surface and subsurface soil moisture expressed as % by volume.

Day	Surface Moisture	Subsurface Moisture
June 20	55	59
July 11	62	68
July 12	66	71
July 21	72	75
July 27	70	77
August 1	67	63
August 10	59	66

Table 4.3: Energy, radiation and water balance components. Energy and radiation units are W m^{-2}. The water deficit is expressed as $\sum$P-E (mm d^{-1}) for each Period.

	Seasonal	**Period I**	**Period II**	**Period III**
Q^*	125.6	166.3	129.2	70.5
Q_E	61.8	102.4	56.8	32.2
Q_H	50.2	48.2	56.9	27.7
Q_G	13.8	18.6	14.7	8.7
β	0.81	0.47	1.00	0.86
KI	225.6	283.7	224.0	147.4
Water Deficit	-105.8	-28.7	-63.6	15.5

Over the full measurement period, the water table averaged -0.22 m and varied between 0.04 and -0.44 m (Figure 4.2a). The water table was closest to the surface in Period I at -0.06 m, whereas in Periods II and III it was -0.26 and -0.27 m respectively. There were three distinct drawdown events over the measurement period. These extreme moisture conditions caused severe cracking and slumping of the peat surface (Figure 4.4).

4.1.3 Vegetation

From the first measurements on June 16 when shoot lengths of the sedges were 7.3 cm, the rate of elongation was linear until the maximum length of 17.7 cm was reached on July 27 (Figure 4.5a). Shoot density ranged from 704 shoots m^{-2} at the beginning of the study period to a maximum density of 1008 shoots m^{-2} by July 28 (Figure 4.5b). The single-sided leaf area index at the beginning of the period was 0.11 and reached a maximum of 0.3 on July 13 (Figure 4.5c).

Successful measurements of stomatal conductance could only be taken between July 8 and July 29 because the sedge leaves must be large enough to sample with a porometer and because leaf senescence started at the beginning of August. The average g_s over this period was 0.78 cm s^{-1}. There was no seasonal trend which would reveal a preferential growth stage for photosynthesis.

FIGURE 4.4: Severe desiccation of the soil surface.

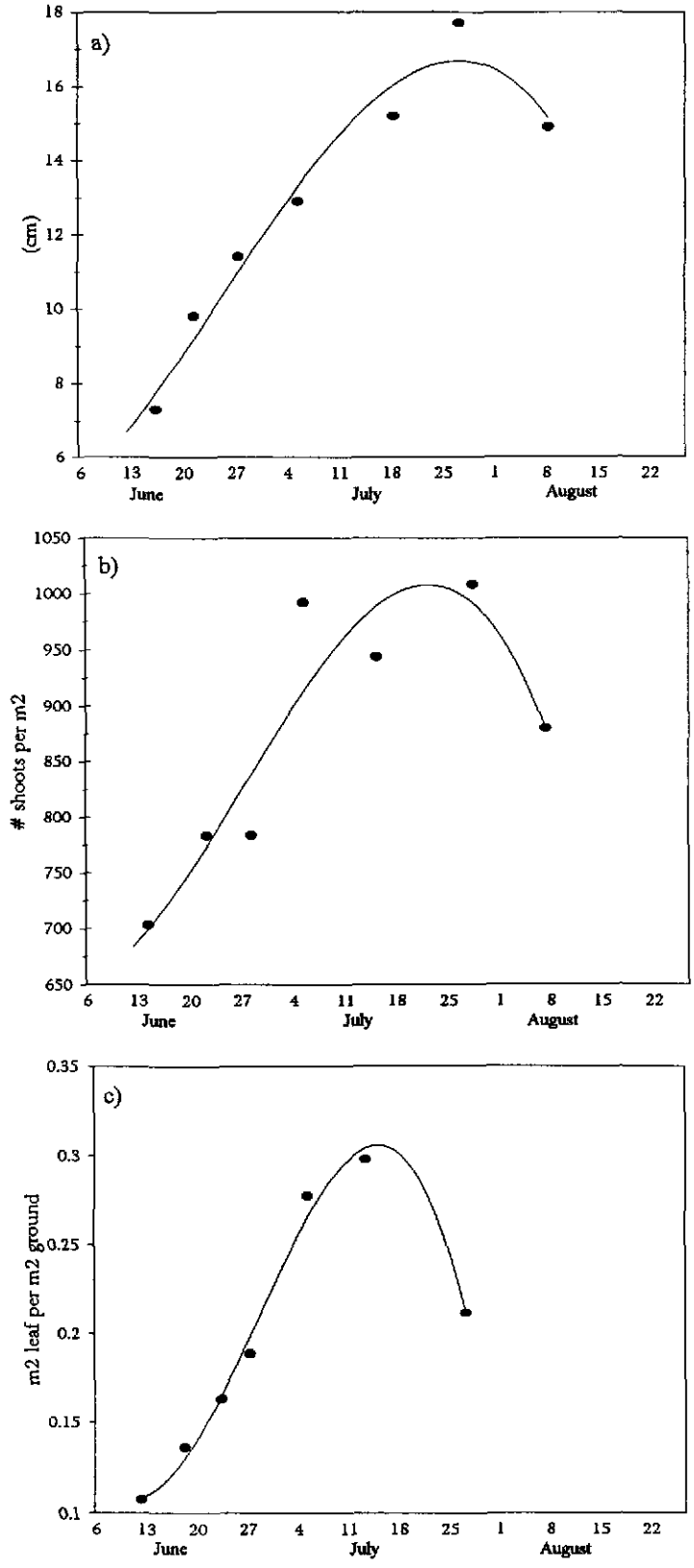

Figure 4.5: Vegetation growth parameters a) shoot length, b) shoot density and c) LAI.

There was, however a distinct diurnal pattern of g_s (Figure 4.6). g_s peaked in the early morning when environmental stresses were small and plants could take advantage of early light to photosynthesize. Subsequently, g_s steadily declined and reached its lowest value at 1200 h and stayed low to 1400 h. At this time, solar radiation was large and evaporative demand high thus inducing plant moisture stress. A secondary mid-afternoon peak was reached at 1500 h when environmental stresses decreased. This pattern is consistent with a Type II pattern of stomatal conductance described by Blanken, (1992). The coefficient of variation for the 6 days was 40 % indicating some variation in response to changing day to day environmental conditions but also indicating a reliable and consistent diurnal trend.

4.2 Carbon Dioxide Fluxes

4.2.1 Diurnal Patterns of Carbon Dioxide Exchange

The average seasonal diurnal pattern of CO_2 flux is shown in Figure 4.7 where each half-hour value is the average of approximately 75 half-hour periods. The curve exhibits a typical pattern of diurnal CO_2 flux in which respiration is dominant in the early morning and late evening hours when photosynthesis does not occur, and where net negative ecosystem exchange is dominant during the day. The average diurnal flux over the season was 0.03

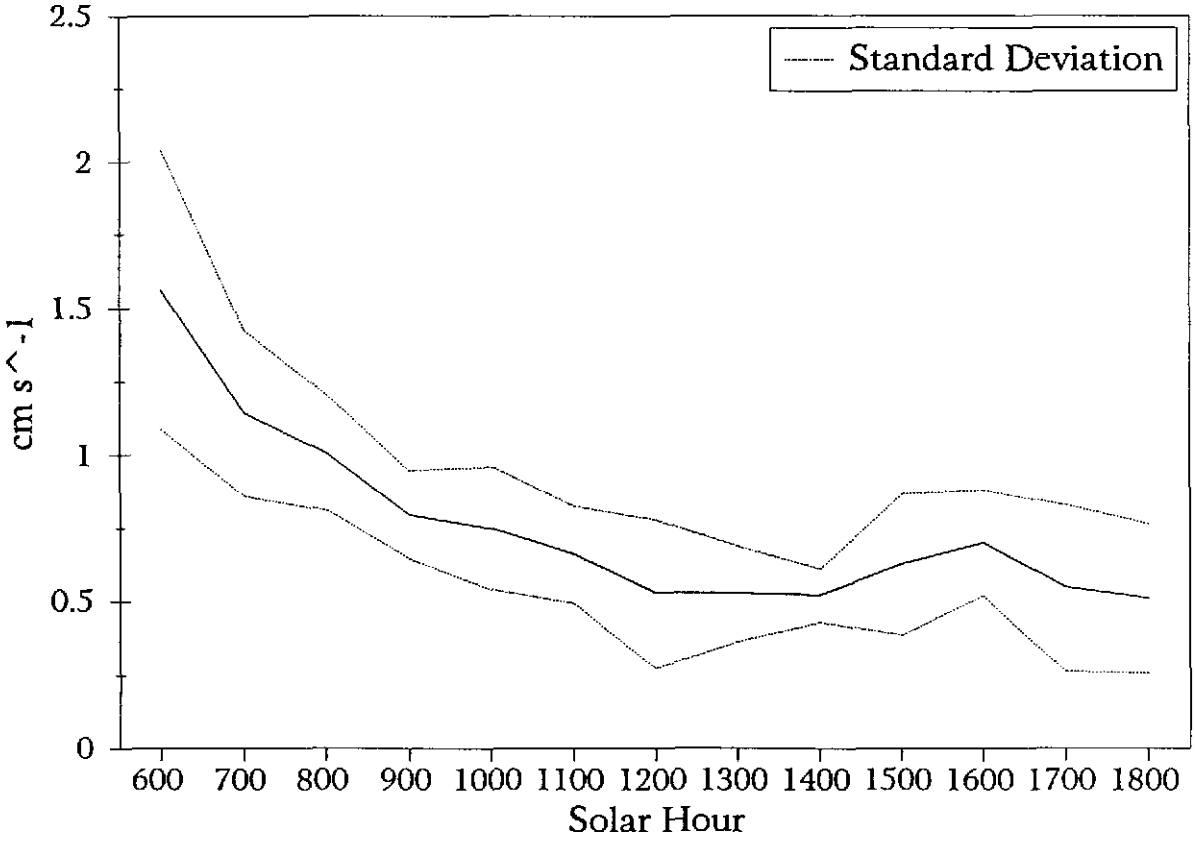

Figure 4.6: Average diurnal pattern of sedge g_s averaged for 6 days during the growing season.

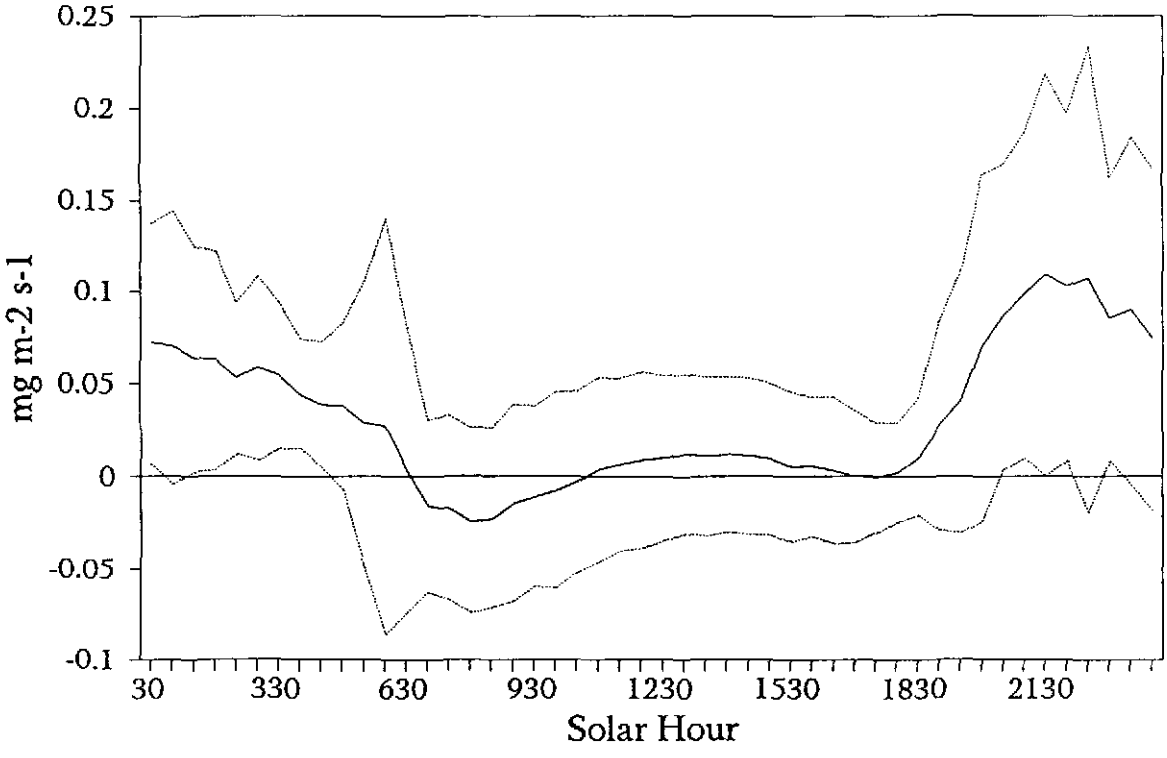

Figure 4.7: Average diurnal curve of CO_2 flux.

mg m^{-2} s^{-1} with a maximum net uptake of 0.02 mg m^{-2} s^{-1} occurring in the morning at 0800 h and a maximum net respiration of 0.11 mg m^{-2} s^{-1} occurring at night between 2130 h and 2230 h. The midday period from 1100 h to 1730 h indicates a net positive ecosystem exchange. Peak fluxes of K↓ and high evaporative demand create a large moisture stress accompanied by decreased stomatal conductance (Figure 4.6) which suppresses photosynthesis therefore causing absolute respiration to dominate. There was also a late-afternoon recovery of absolute photosynthesis (1700 h to 1800 h) which coincided with the increase in g_s shown in Figure 4.6. Similar diurnal patterns are reported by Neumann *et al.* (1994) for a raised open bog in the southern Hudson Bay Lowland except that they show a daytime dominance of photosynthesis.

The different diurnal patterns in Periods I, II and III (Figure 4.8) reflect the role of vegetation in determining the net fluxes. During Period I, the average diurnal curve exhibited no daylight periods for which there were net photosynthetic (negative) fluxes (Figure 4.8a). However, the net ecosystem exchange during the day was 36 % smaller than the exchange during the night (Table 4.4) which indicates that even though the vegetation canopy was sparse, it was fixing CO_2. Maximum daytime and nighttime positive exchange occurred at 0600 h and 2130 h, respectively. At 0600 h, fluxes of Q_G and Q_H changed from being negative to positive, while sunset occurred at 2130 h. The nighttime flux was 21 % and 42 % larger than the nighttime fluxes for Periods II and III respectively. During the maximum growth period, there was a net photosynthetic (negative flux) uptake of CO_2 during the day (Figure 4.8b). Peak negative net exchange occurred at 0800 h with a steady

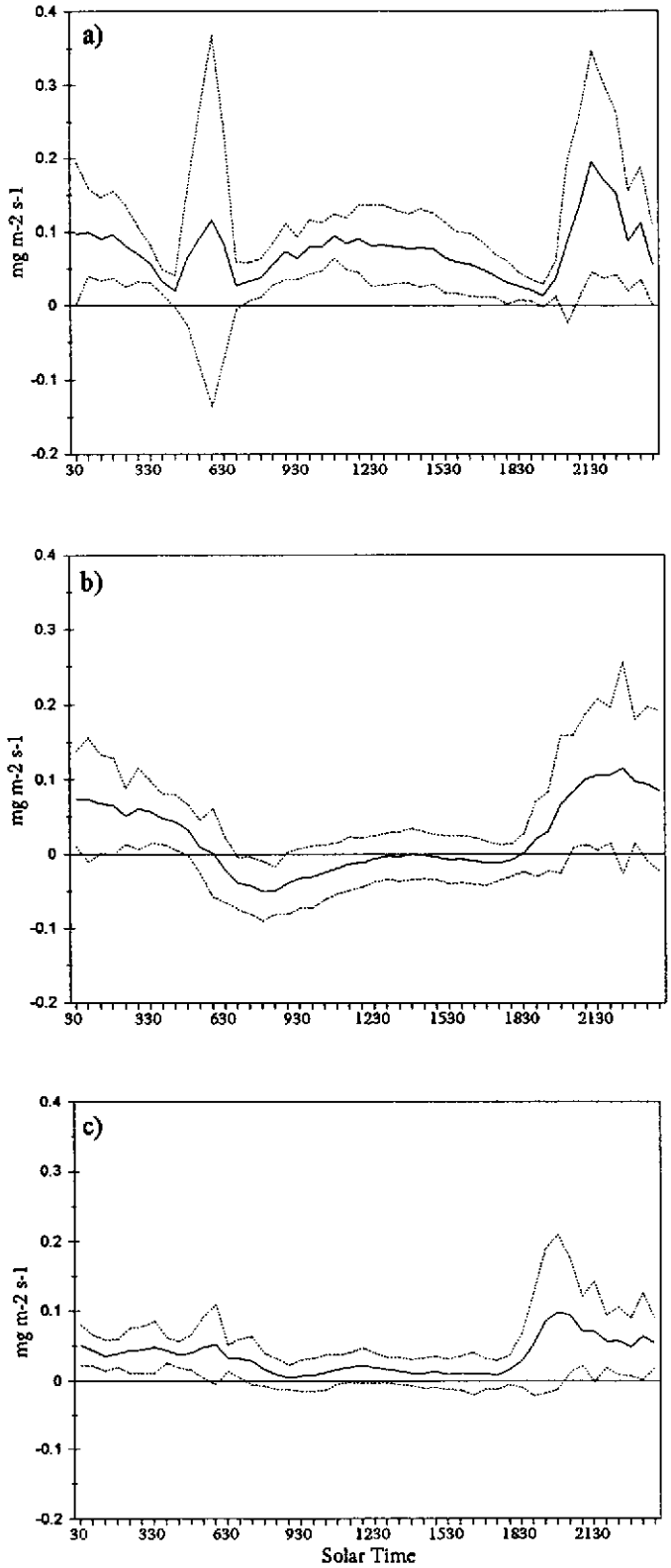

Figure 4.8: Diurnal fluxes of CO_2 during a) Period I, b) Period II and c) Period III. The dotted line represents the standard deviation.

Table 4.4: Diurnal means of CO_2 (mg m^{-2} s^{-1}). Negative values denote net photosynthetic exchange.

	Period I	**Period II**	**Period III**
Diurnal mean	0.074	0.021	0.034
Day	0.062	-0.012	0.018
Night	0.097	0.077	0.056

decrease to early afternoon followed by a small recovery at 1700 h. The largest absolute respiration occurred at 2230 h.Period III was characterized by leaf senescence and exhibited no net negative exchange of CO_2 (Figure 4.8c). The largest net respiration fluxes occurred at 0600 h and 2000 h.

4.2.2. Seasonal Patterns of Carbon Dioxide Exchange

The seasonal daily averages are illustrated in Figure 4.9. On a daily basis, this sedge fen showed a large net efflux of CO_2 in 1994. Only three days over the entire season exhibited a net daily uptake. On average, 0.03 mg CO_2 m^{-2} s^{-1} was emitted into the atmosphere over the entire season. Period I showed the largest daily emission which was on average 64% greater than the fluxes during Periods II and III (Table 4.5). This was due to little or no photosynthetic uptake by vegetation.

To interpret these patterns, daytime and nighttime fluxes are separated. Figure 4.10a shows the daytime fluxes ($Q^*>0$). Period I showed high respiration and no days for which net negative exchange dominated. This is because the vegetation canopy was not yet fully established. In Period II, the daytime fluxes were dominated by net photosynthesis. Respiration may still have been large, but was offset by larger photosynthesis. On 10 days in Period II, there was net respiration. On 5 of these days, photosynthesis was suppressed by rain events and low $K\downarrow$. One of the days was at the beginning of the Period when the vegetation canopy may still have been sparse. The other 4 days had very high $K\downarrow$ which

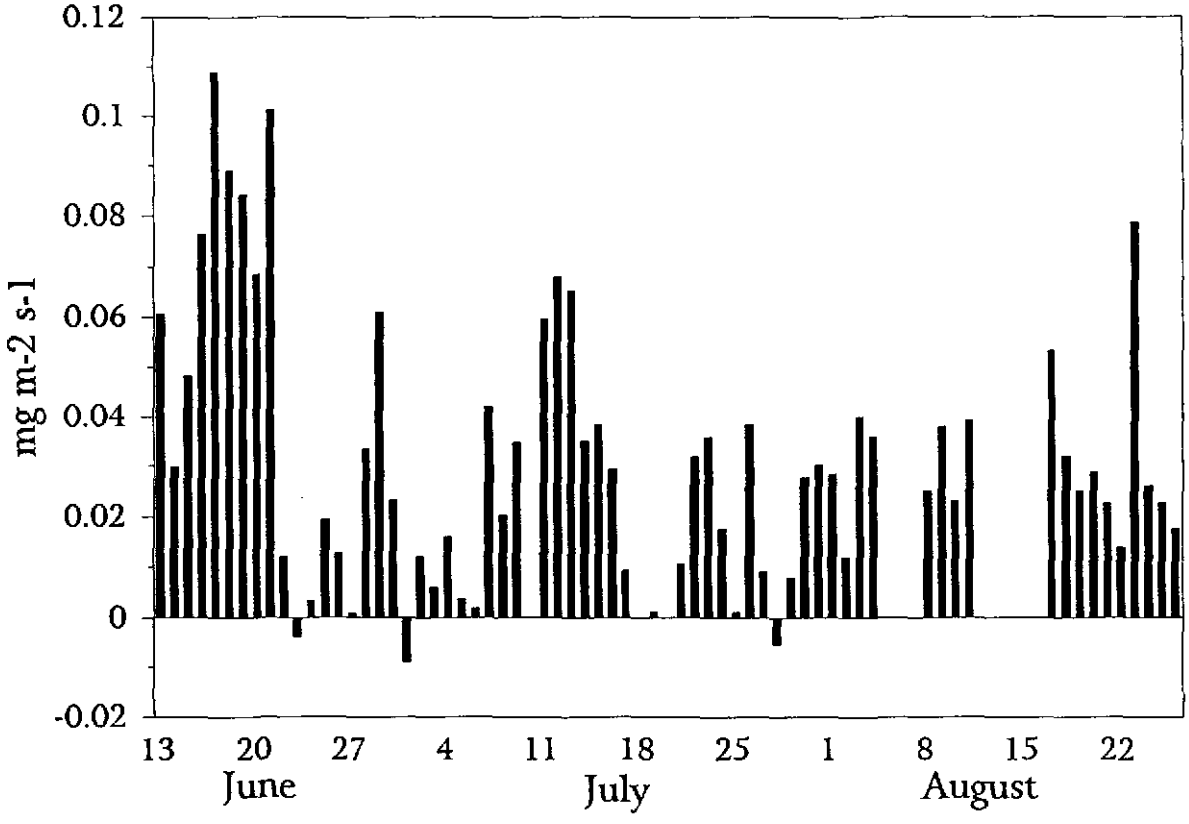

Figure 4.9: Daily average CO_2 flux.

Table 4.5: Average CO_2 fluxes (mg m^{-2} s^{-1}). Negative values denote net photosynthetic exchange.

	Seasonal	**Period I**	**Period II**	**Period III**
Daily	0.031	0.074	0.022	0.032
Day	0.004	0.062	-0.011	0.017
Night	0.074	0.097	0.076	0.060
g CO_2 m^{-2} d^{-1}	2.7	6.4	1.9	2.8
g CO_2 m^{-2}	175.1	57.6	81.2	36.3

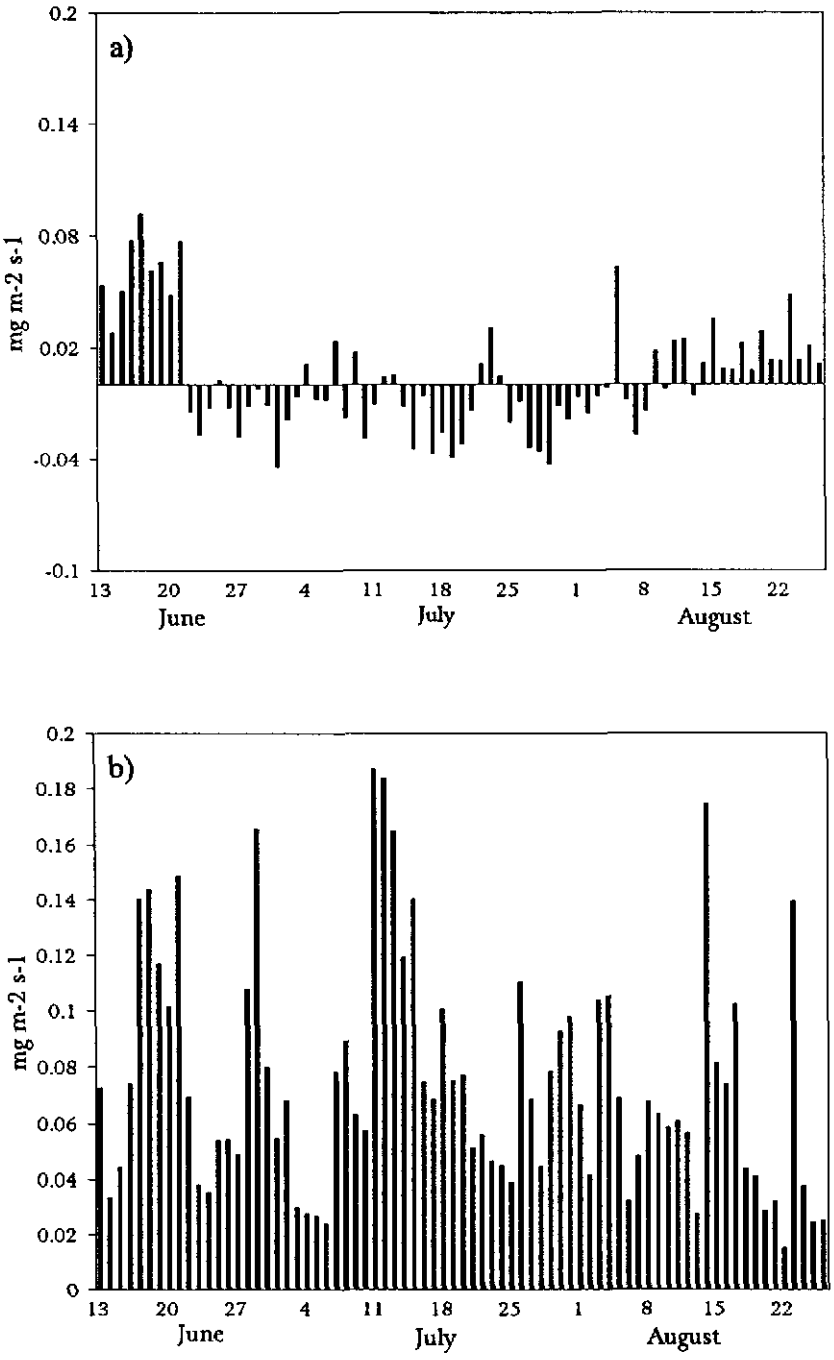

Figure 4.10: Average a) daytime and b) nighttime CO_2 exchange.

could indicate that an optimal level of K↓ for photosynthesis was exceeded. In Period III, there was net positive ecosystem exchange on all but 2 days. The net respiration was smaller than in Period I probably because some living vegetation was still contributing to photosynthesis and because the water table rose due to rain events.

The nighttime fluxes ($Q^{*}<0$) are shown in Figure 4.10b. The largest respiration occurred during Period I which had fluxes 30% larger than during Periods II and greater than in Period III.

The mean fluxes for the 3 Periods were quite different (Table 4.5) and can be explained by vegetation development. Table 4.6 compiles fluxes reported for various locations. Large fluxes were reported in studies 1, 2 and 3. In 1, the conditions of a drained peatland in a temperate climate would be conducive to large effluxes of CO_2. This study does not report on net ecosystem exchange but on CO_2 emissions from the soil environment only. Large fluxes for 2 and 3 seem to be related to location/regional conditions or to dynamic chamber methods which may underestimate photosynthetic uptake. Results from 5 showed similar trends to the present study with larger photosynthetic uptake during the day probably as a result of a denser vegetation canopy. While studies 6 and 7 showed similar magnitudes of fluxes, only study 6 illustrated the effects of moisture with tussock tundra having larger fluxes. Studies 9, 10 and 11 clearly illustrate the influence of soil moisture on CO_2 exchange. When comparing study 8 to the present study, it showed evidence of larger ecosystem uptake during the growing season but smaller CO_2 efflux during the early and late seasons. This could be attributed to a denser vegetation cover.

Table 4.6: Comparative studies of CO_2 fluxes..

Authors	Location	Peatland Description	Methods	CO_2 Flux ($g\ m^{-2}\ d^{-1}$)
1) Glenn *et al.*, 1993	Napierville, Que	drained peatland	static chamber	1) 0 to 16
2) Oberbauer, *et al.*, 1991	Imnavait creek watershed, Alaska	1) tussock tundra 2) water track	dynamic chamber	1) ~5.7 to 10.6 2) ~4.6 to 11.8
3) Oberbauer, *et al.*, 1992	Imnavait creek, Alaska June 18 to July 24	riparian community 1) *Carex* 2) *Eriophorum*	dynamic chamber	1) 4.8 to 11.0 2) 1.0 to 9.0
4) Schreader, 1994	Churchill, MB June, July, Aug.	sedge fen	BREB	6.4 late June 1.9 peak season 2.8 senescence
5) Neumann *et al.*, 1994	Lake Kinosheo, southern HBL	raised open bog	1) EC 2) BREB	1) -2.93 day 2.67 night 2) -3.32 day 3.67 night
6) Poole and Miller, 1982	July and August north-central Alaska	1) tussock tundra 2) shrub tundra 3) lichen-heath	static chamber	1) 2.3 2) 1.4 3) 1.7
7) Whiting *et al.*, 1992	Bethel, Alaska July 8 to Aug. 8	1) wet meadow 2) dry upland tundra	dynamic chamber and EC	1) 1.9 2) 1.0
8) Coyne and Kelly, 1971	Barrow, Alaska July and August	tundra	aerodynamic	1.0 late June - 8.0 peak season 1.5 senescence
9) Moore, 1989	Schefferville, Que May to Oct, 1987	patterned fen 1) pool 2) flark 3) string	static chamber	1) ~0.1 to 0.6 2) ~0.2 to 5 3) ~0.25 to 6.2
10) Burton *et al.*, 1995	Churchill, MB July, August	sedge fen	BREB	3.62 dry 0.34 wet
11) Oechel *et al.*, 1993	Toolik Lake, Alaska Summer 1983-1987,1990	1) tussock tundra 2) wet sedge 3) wet/moist sedge	dynamic chamber gas exchange system	1) 0.72 - 3.9 2) 0.03 - 0.66 3) 0.09 / 0.31

The study by Burton *et al.*, (1995) offers a direct comparison of CO_2 fluxes for the same site and measurement methodology. Burton *et al.* (1995) reported an average seasonal flux of 0.01 mg m^{-2} s^{-1} from the mid-summer period July 11 to August 29. Similarly, for a season which mostly represents the maximum growth period, this fen experienced a net loss of CO_2, the magnitude of which was smaller in comparison to the present study. This can be attributed to a water table which was on average 0.08 m higher. The 'wet' and 'dry' fluxes from Burton's study are not directlly comparable to the present study because the mean water table depth and range were much smaller.

4.3 Environmental Controls

4.3.1 Temperature

In Period I, there was a distinctive response to surface temperature both by day and night (Figure 4.11). There were also similar responses to air and subsurface temperatures. Daytime net positive exchange became larger with increasing temperature to an optimum level beyond which fluxes decreased. At night there was a linear response of increasing absolute respiration to increasing temperatures.

Because of the sedge growth in Period II, daytime fluxes were divided into those which were dominated by photosynthesis (negative net exchange) and those which were dominated by respiration (positive net exchange). Net negative exchange was not correlated

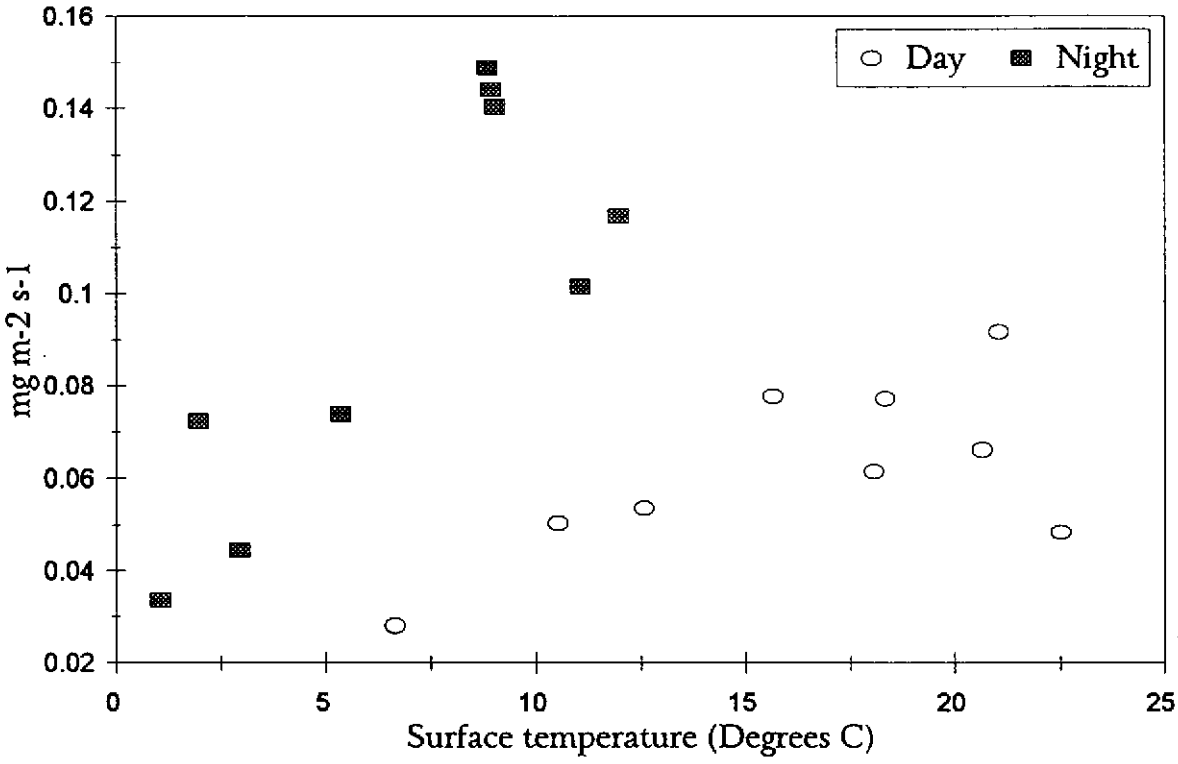

Figure 4.11: The effects of surface temperature on daytime and nighttime fluxes of CO_2 during Period I.

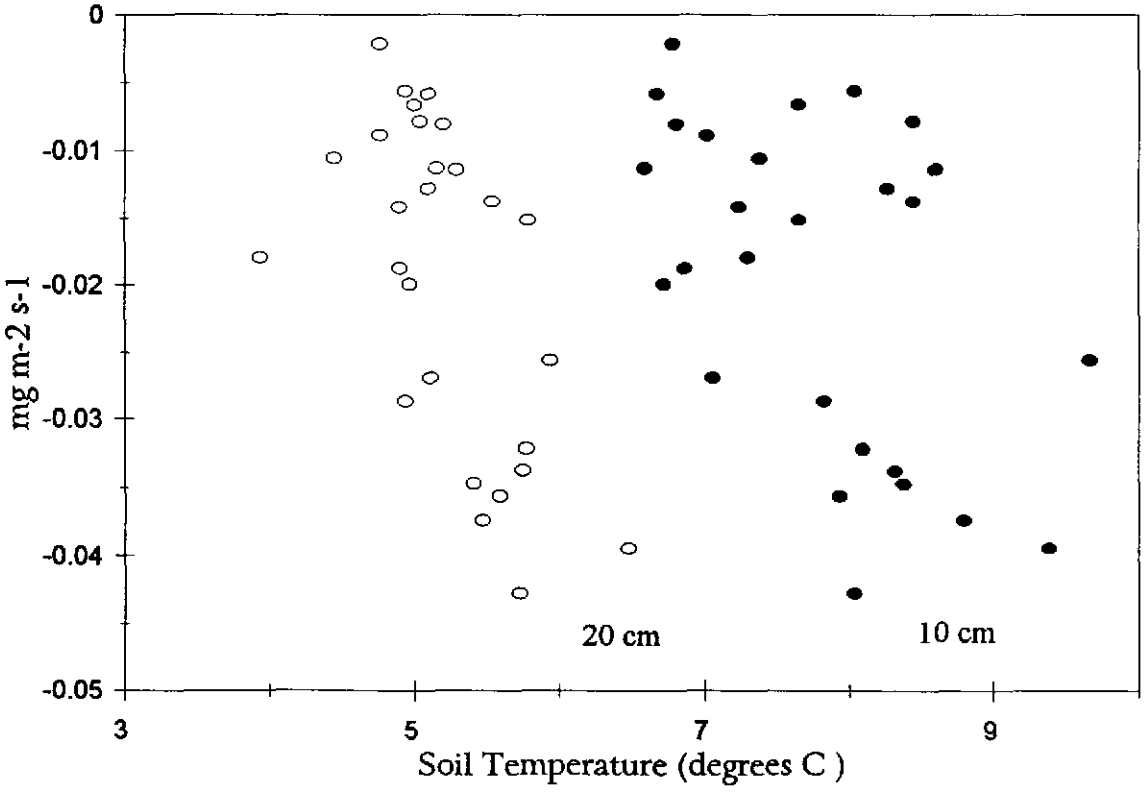

Figure 4.12: Influence of temperature at different soil depths on net negative exchange during Period II.

with daytime temperatures. However, 71% of these fluxes occurred when soil temperatures were <10.0 °C at a depth of 0.1 m and < 6.5 °C at a depth of 0.2 m. These fluxes became increasingly negative (photosynthesis increased) as temperatures increased (Figure 4.12). Daytime net positive exchange during Period II did not seem to be related to temperature. Rather, these fluxes were due to rain events, and extremes of K↓ which may have suppressed the absolute photosynthetic flux. Nighttime fluxes during this Period did not exhibit a relationship with temperature. Neither daytime nor nighttime fluxes in Period III were related to temperature.

Weak relationships between temperature and fluxes may be due to variable responses over a wide range of temperatures. It has been shown that when vegetation was minimal both daytime and nighttime fluxes increased with temperature to a maximum temperature. Also, during the maximum growth period, net negative exchange during the day increased with temperature for a specific range of temperatures. Different magnitudes of absolute photosynthesis and respiration may have different response curves to temperature. One way to investigate this is to examine the relationship between temperature and different magnitudes of fluxes. For nighttime fluxes <0.05 mg m^{-2} s^{-1}, there was a positive linear response to surface temperatures for Periods I and II. With larger fluxes, there was a negative linear relationship with surface temperature. This trend is consistent with soil temperatures at a 0.10 m depth. These findings are consistent with the optimal response curve shown for Period I.

4.3.2 Water Table Depth

During Period I, both daytime and nighttime fluxes increased with increasing water table depth to an optimum depth, after which both fluxes decreased despite further increases in water table depth (Figure 4.13). This was similar to the flux response to temperature. The maximum daytime flux occurred at a water table depth of ~0.05 m while the maximum nighttime flux occurred at water table depth of ~0.07 m.

During Period II, daytime fluxes which exhibit net positive exchange showed a curvilinear increase of flux with an increase in water table depth. No correlation was evident for daytime net negative exchange or nighttime fluxes. Fluxes in Period III did not exhibit any relationship with water table depth during the day or night.

Analysis thus far has shown inconsistent responses to the common environmental controls normally examined in carbon budget studies except during Period I. This data set should provide ideal circumstances to quantify the relationship between water table position and CO_2 flux because of the large range in water table depths over the season. There were three distinct drawdown periods over the season. Figure 4.14 shows the significant responses of CO_2 fluxes to changes in water table depth over these periods. The first drawdown occurred at the beginning of the study period from June 13 to July 2 when the water table dropped from -0.01 m to -0.18 m. The net flux decreased with increasing water table depth. This period overlaps with the vegetation period, therefore, it appears that opposing responses of absolute photosynthesis and respiration may be confusing the trend.

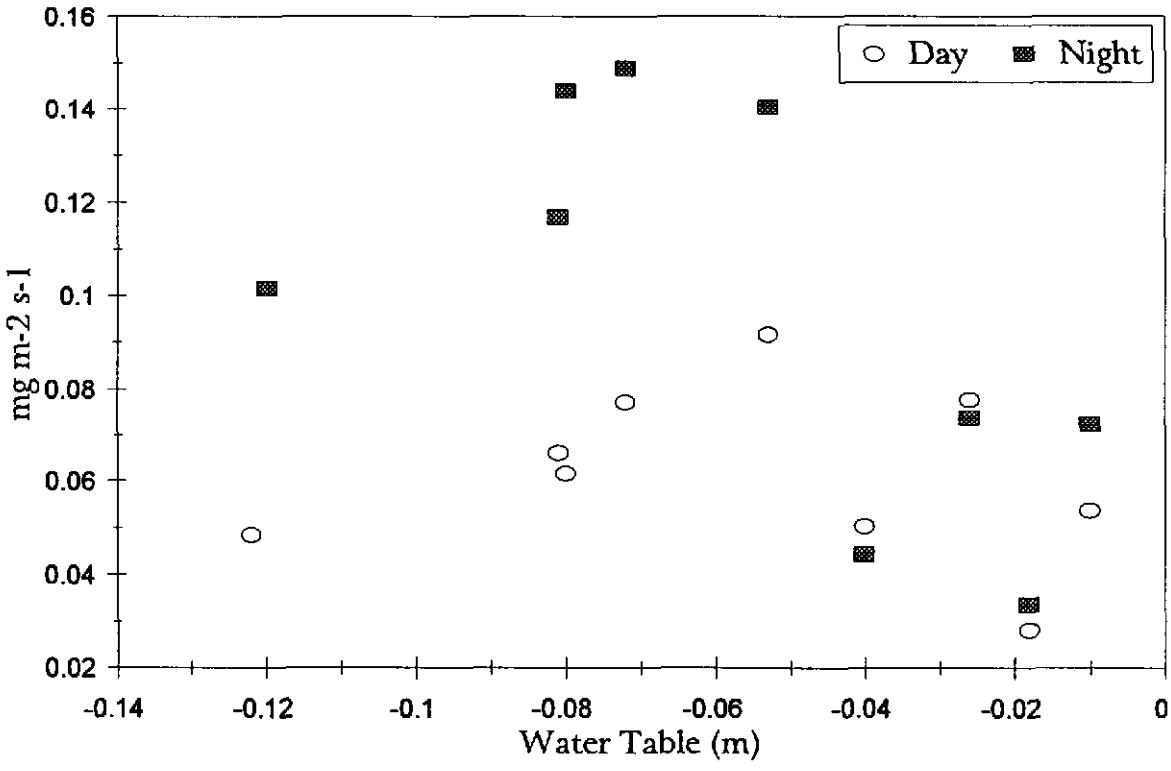

Figure 4.13: The effects of water table depth on daytime and nighttime fluxes during Period I.

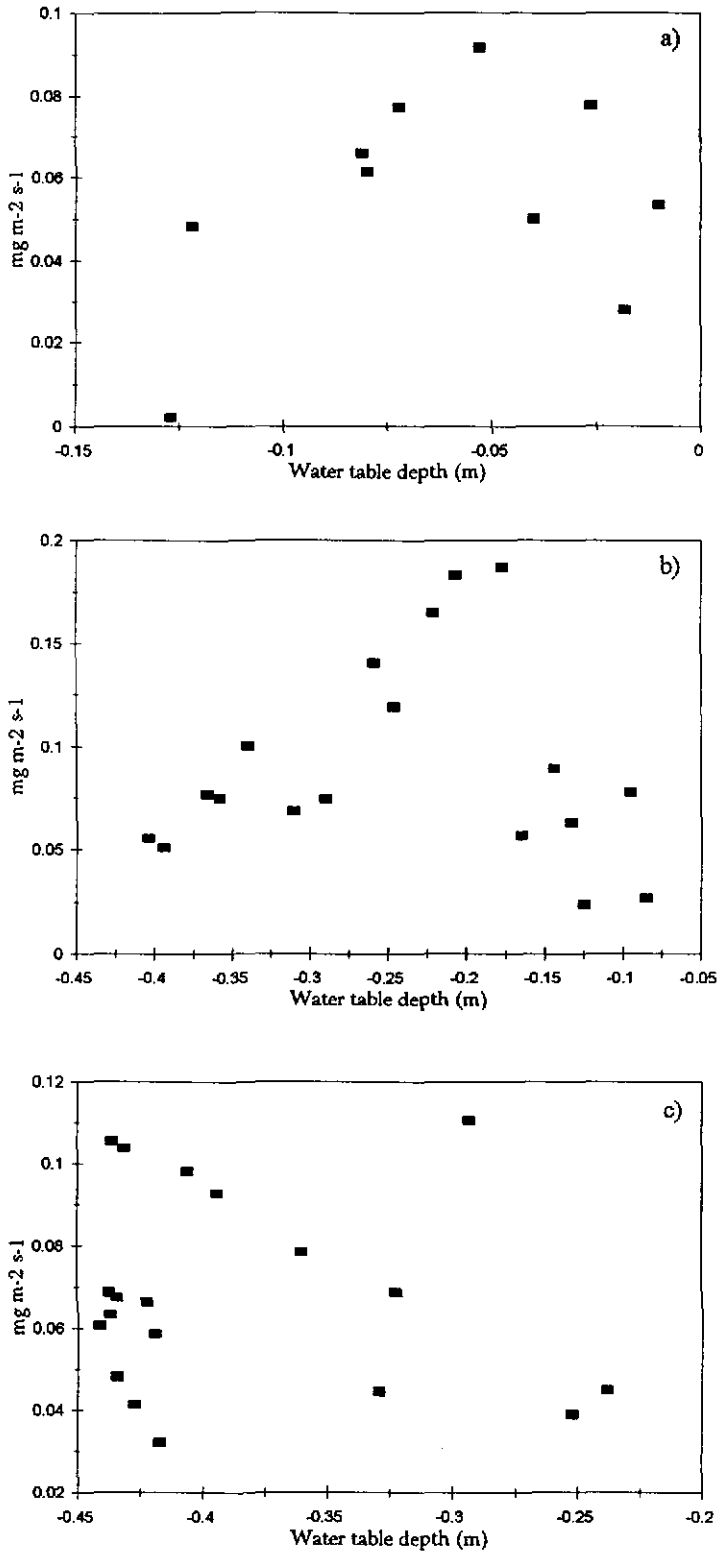

Figure 4.14: Response of CO_2 flux during drawdown periods a) June 13 to July 2, b) July 5 to July 22 and c) July 24 to August 11.

Within the overall daily pattern, the nighttime fluxes showed no clear response to this drawdown, while positive daytime fluxes clearly increased with the water table depth to 5 cm, then decreased as the water table receeded further (Figure 4.14a). No trend was evident for negative daytime exchange.

The second drawdown period occurred over the first part of Period II extending from July 5 to July 22. Nighttime fluxes displayed the optimal response pattern increasing as the water table lowered to approximately -0.13 m and then decreasing linearly with increasing water table depth. The net and daytime fluxes did not show any relation to water table recession.

The third drawdown period extended from July 24 to August 11 and thus mainly occurred in Period II but slightly overlapped into Period III. It did not influence net or daytime fluxes. There was a weak optimal response with nighttime fluxes consistent with the other two drawdown periods. Fluxes increased to water table depths of -0.44 m, and then decreased sharply.

This optimal response was also reported by Hogg *et al.*, (1992). Although CO_2 production was greater in drained peat profiles, respiration increased during drying cycles, but tended to decrease when very dry conditions were reached. These authors found that CO_2 emission rates from the 0-10 cm depth were 2 to 4 times greater than from the 10-20 cm depth and 4 to 9 times greater than from the 30-40 cm depth even after 3 months exposure to aerated conditions and warm temperatures. This is attributed to a greater abundance of freshly killed plant biomass on the surface and an accumulation of unfavourable

components (lignins and humic substances) in the deeper peat layers which would suppress biological activity. The intrinsic chemical and physical characteristics of certain peat-forming plants, such as *Sphagnum* may also lead to decay-resistant peat (Johnson and Damman, 1991). The notion of decay-resistant organic material becomes very important in climate change studies. Generally, it is thought that warmer and drier conditions will be conducive to larger amounts of CO_2 being evolved from deeper soil strata. However, a resistance to decay at these depths makes the CO_2 evolution less sensitive to environmental changes.

The difficulty of quantifying relationships between ecosystem CO_2 exchange and environmental influences has been clearly demonstrated. Controlled laboratory experiments have proved more successful than field studies, where isolating the effects of a particular environmental variable varies from difficult to impossible. Temperature and water table depth have been identified as the largest controls on CO_2 exchange. However, the response of the CO_2 flux to one variable may be dependent on the magnitude of the other variable. Following the analysis of Kim and Verma (1992), attempts were made to quantify this.

Daytime and nighttime fluxes were plotted against water table depth under different conditions of surface temperature and, against surface temperature for different ranges of water table depth. Distinct differences in flux responses were found for extremes of water table depth and surface temperature. Figure 4.15a illustrates that when the water table was high, positive net exchange during the day increased with increasing surface temperature. However, when the water table was low, these fluxes decreased as surface temperatures increased. The water table was generally low during the growing season, when daytime

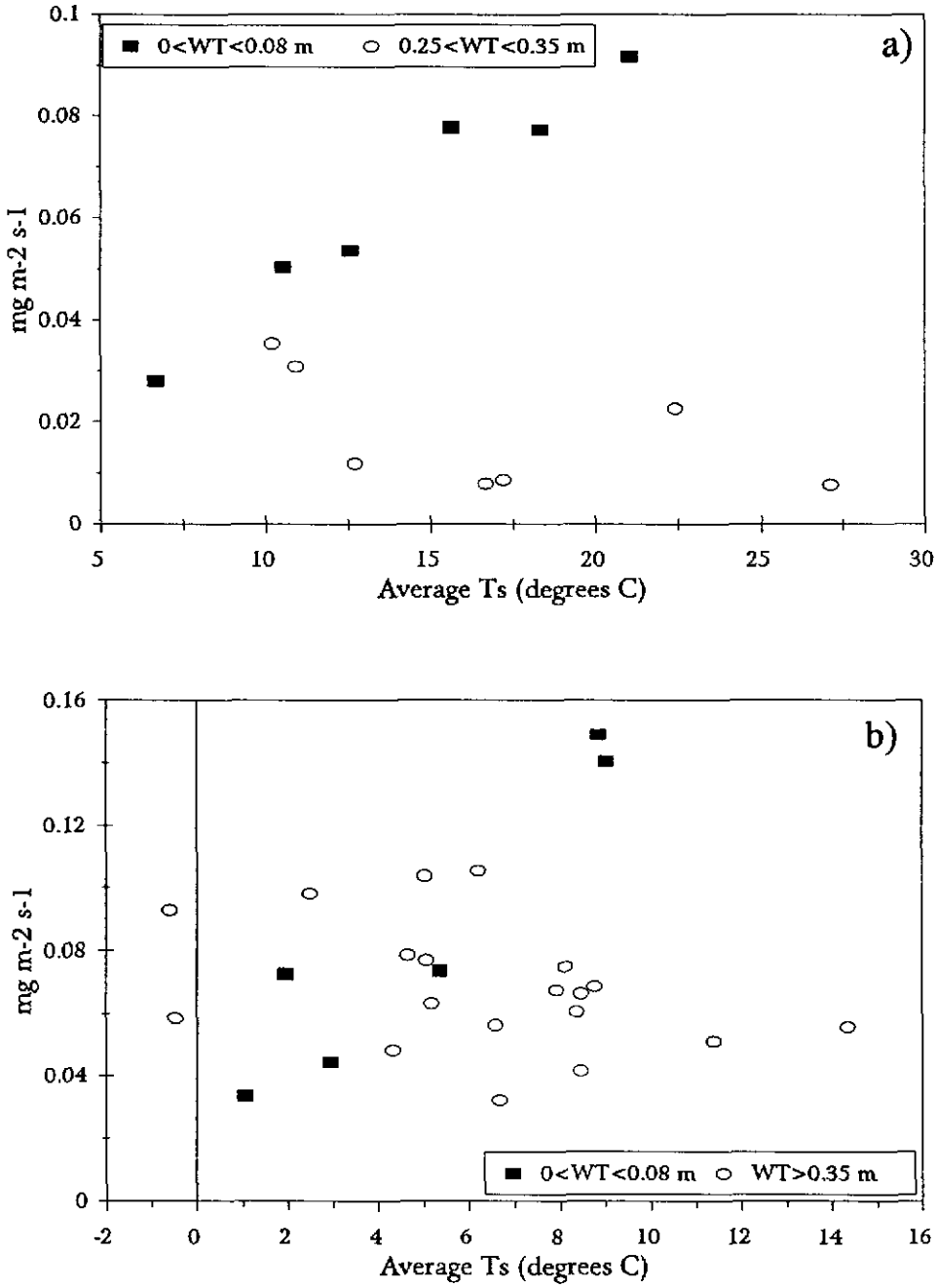

Figure 4.15: Response to temperature under extremes of water table depth during a) the day and b) the night.

fluxes would tend toward negative ecosystem exchange, especially under warmer conditions. This would make postive net ecosystem exchange smaller. However, nighttime fluxes exhibited the same trend (Figure 4.15b). One explanation may be that plant respiration is being limited by lower soil moisture. Results from Hogg, *et al.* (1992) also demonstrate the different effect of temperature on CO_2 flux at different levels of saturation. For drained peat cores, CO_2 emissions increased exponentially with temperature. However, there was a much weaker response of fluxes to increasing temperature when samples were flooded, because oxygen is still necessary for microbial activity.

Daytime fluxes showed the same response to water table fluctuations over a range of surface temperatures (Figure 4.16a). Nighttime fluxes showed different responses to water table depth at different ranges of surface temperatures. When surface temperatures were low, fluxes increased with water table depth. When surface temperatures were moderate, fluxes decreased with increasing water table depth (Figure 4.16b).

Daytime fluxes also showed a differential response to water table depth under different ranges of solar radiation (Figure 4.17). When incoming solar radiation was low, fluxes generally increased with water table depths greater than -0.20 m. Positive exchange decreased with increasing water table depth when incoming solar radiation was large. This may have been due to optimal photosynthesis (negative fluxes) occurring at K↓ values close to 350 W m^{-2}.

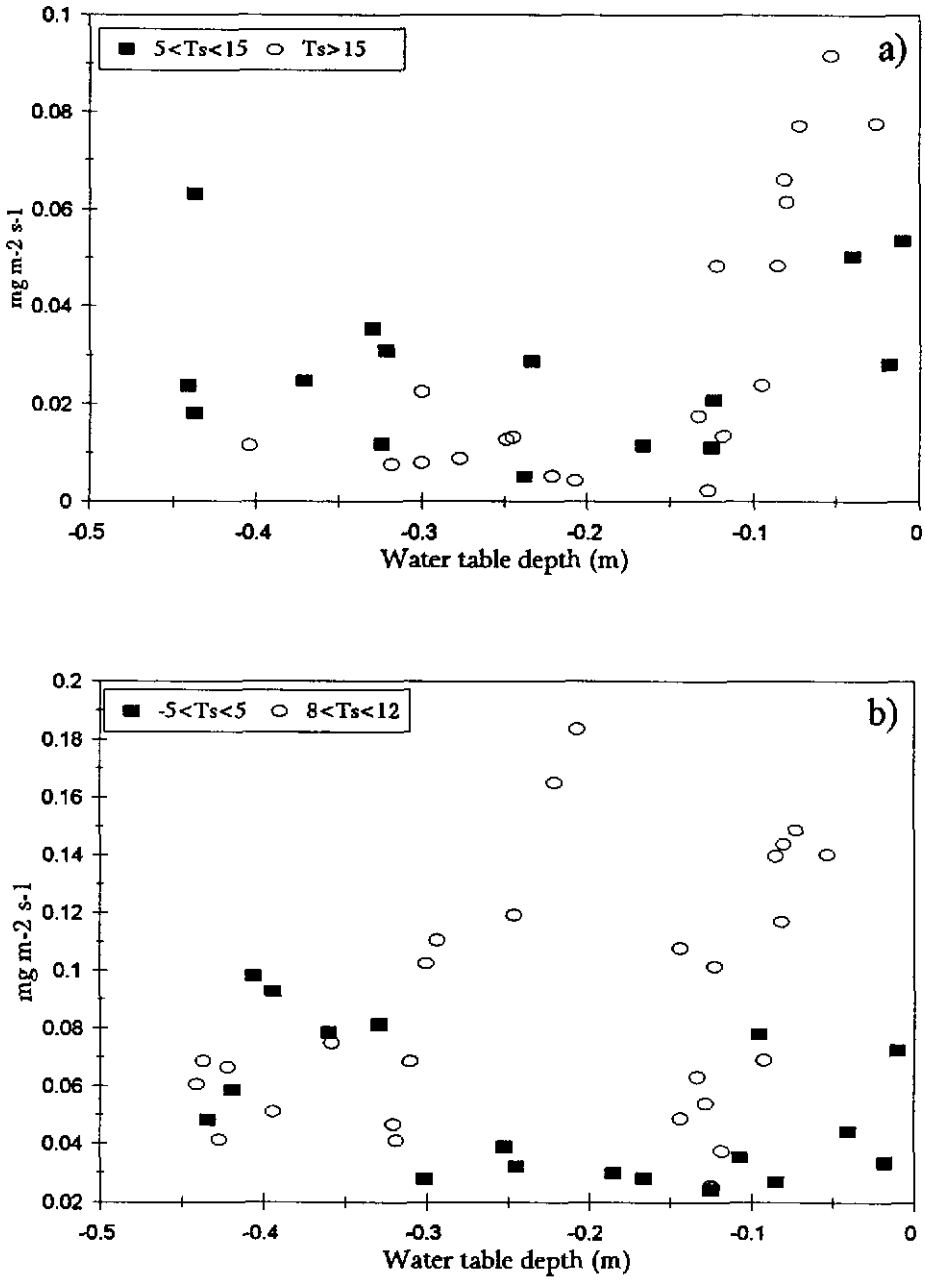

Figure 4.16: Responses to water table at different ranges of temperature during a) the day and b) the night.

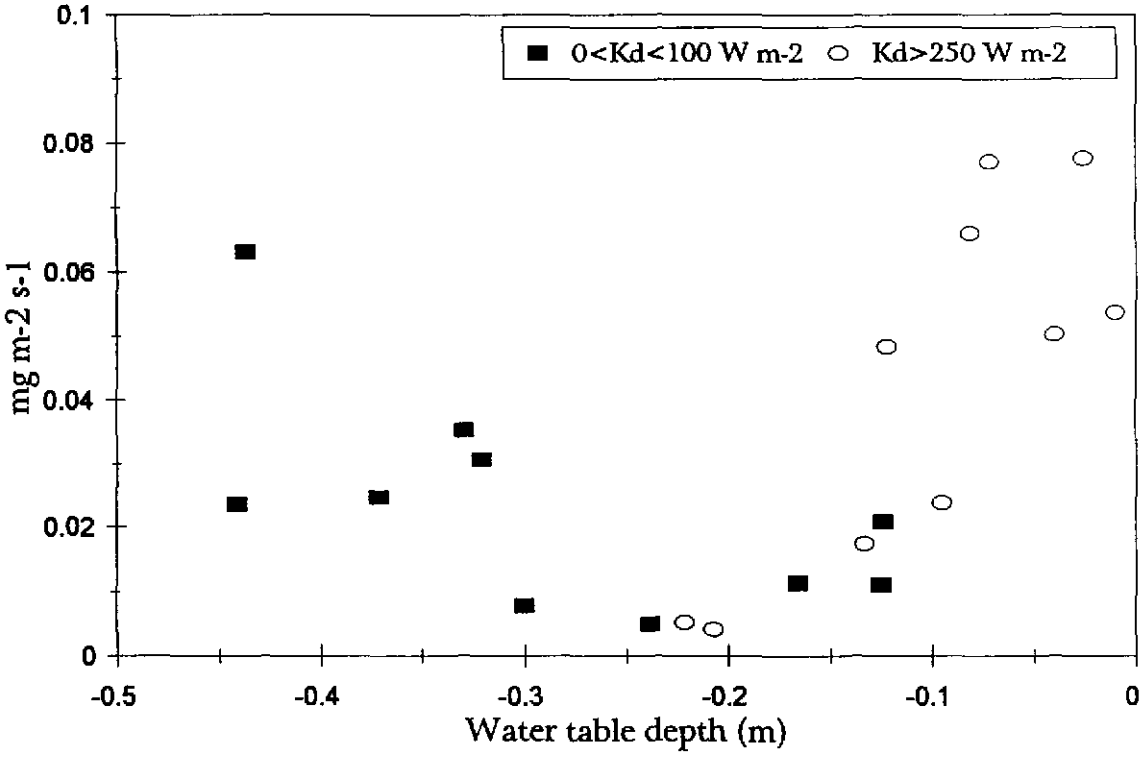

Figure 4.17: Responses to water table depth at different levels of K↓.

Chapter 5

Summary and Conclusions

5.1 Significant Conclusions

The most significant factor in controlling the exchange of CO_2 from this ecosystem is vegetation. This is evident in Period II, when the magnitude of daily net fluxes is reduced by the daytime photosynthetic assimilation of CO_2. Since the maximum growth period in this northern location is short (approximately 6 weeks), seasonal uptake of CO_2 is minimal. Even in the maximum growth season, this fen experienced a net loss of CO_2. This suggested that other environmental factors must also play a large role in controlling fluxes. This season was drier and warmer than normal and thus more conducive to soil respiration. However, Burton , *et al.* (1995) reported a net loss of CO_2 for this site under wetter conditions. It follows that the vegetation canopy is not substantial enough for this site to be a net sink for CO_2, even under conditions which would suppress respiration. Assuming that biological succession has progressed gradually with emergence from the coast, at no time in the past would there have been a denser vegetation canopy at this site. The present accumulation of peat could be from previous coastal deposits of seaweed and kelp. This would imply that

that this site has always been a net source for CO_2. On the other hand, non-vascular species such as mosses, may represent a large historical sink for CO_2 and explain the accumulation of peat. Age profiles of the peat could reveal the origin of accumulation at this site.

Although predictions of climate change suggest warmer and drier conditions for this region, abnormally dry conditions during this season did not contribute to an exceptionally larger amount of CO_2 being evolved. Analyses of environmental controls revealed that CO_2 exchange followed an optimum response curve to surface temperature and water table depth. This translates into an upper limit of CO_2 evolution for this region. The dry conditions of this season did not promote large increases in soil respiration, therefore is is predicted that future dry seasons will not lead to enhanced CO_2 loss. Warmer temperatures generally increase metabolic activity. Results from this study suggest that, there is an optimal level of temperature, after which activity is suppressed. Although, the biological processes responsible for this are not fully understood, it does imply that increased global temperatures may not lead to larger CO_2 losses from northern regions. The species-specific responses of plants and organisms to different environmental conditions must be further explored in order to fully investigate this.

5.2 Future Recommendations

It is evident that to achieve a better understanding of the net CO_2 flux dynamics, one must separate streams of photosynthesis and respiration and quantify environmental controls for each. This could be done by employing dynamic chambers or photosynthesis chambers. In this study, only the contribution of sedge species was considered. It has been shown however, that mosses and lichens constitute a large proportion of total surface coverage and therefore represent an important photosynthetic component. Thallophytes, as noted in the introduction, respond quite differently to water and light stress than do vascular plants. An investigation of CO_2 exchange within these species would add insight into the flux response to the environment.

Extending the measurement period to include spring and fall would provide a wider water table range, and a larger range in temperatures (soil warming and soil cooling) in which to study environmental controls.

To investigate the notion of decay-resistant peat, it would be useful to measure CO_2 evolving from different depths within the peat profile. These results would be essential in predicting how this system would respond to elements of climate change.

Appendix

A) The Theory of the Radiation Balance.

The radiation balance at the surface is expressed as:

$$Q^* = K^* + L^* \tag{A.1}$$

where Q^* is the net allwave radiation and K^* and L^* are the net shortwave and longwave radiation respectively. K^* is expressed by:

$$\begin{aligned} K^* &= K\downarrow - K\uparrow \\ &= K\downarrow(1-\alpha) \end{aligned} \tag{A.2}$$

where α is the surface albedo (α=K↑/K↓). L^* is given by:

$$L^* = L\downarrow - L\uparrow \tag{A.3}$$

$L\uparrow$ is described by the Stefan-Boltzman Law and is expressed as:

$$L\uparrow = \epsilon\rho(T_o)^4 \tag{A.4}$$

where ϵ is the surface emissivity, ρ is the Stefan-Boltzman constant and T_o is the surface temperature (°K). Values of ϵ range between 0.90 and 0.99 for agricultural crops and tundra (Oke, 1987) and ρ is 5.67×10^{-8} W m^{-2} K^{-4}.

B) The Theory of the Energy Balance

The Bowen Ratio Approach

The energy balance approach to estimating convective fluxes seeks to apportion the energy available (Q^*) into that used for evaporation, that used to heat the atmosphere and that used to heat the ground. The basic energy balance for an extensive homogeneous surface can be expressed as:

$$Q^* = Q_E + Q_H + Q_G \tag{B.1}$$

where Q_E is the latent heat flux, Q_H is the sensible heat flux and Q_G is the ground heat flux. The vertical flux densities for water vapour and heat are given by:

$$Q_E = -\frac{\rho C_p}{\gamma} K_W \frac{\partial e}{\partial z} \tag{B.2}$$

$$Q_H = -\rho C_p K_H \frac{\partial T_a}{\partial z} \tag{B.3}$$

where ρ is the density of air, C_p is the specific heat of air at constant pressure, K_W and K_H are the turbulent transfer coefficients for water vapour and heat respectively, and γ is the psychrometer constant. γ can be determined by:

$$\gamma = \frac{C_p P}{L_v E} \tag{B.4}$$

where P is the atmospheric pressure, L_v is the latent heat of vaporization and E is the ratio of the molecular weights of water and dry air (0.62).

The ground heat flux (Q_G) can be determined by the following:

$$\begin{aligned} Q_G &= -k_s \frac{\partial T_s}{\partial z} \\ &\approx -k_s \frac{T_2 - T_1}{z_2 - z_1} \end{aligned} \tag{B.5}$$

where k_s is the thermal conductivity of the soil. The sign indicates the flux is in the direction of decreasing temperature.

The Bowen Ratio (β) can be evaluated by:

$$\beta = \frac{Q_H}{Q_E} = \gamma \frac{\partial T}{\partial e} = \gamma \frac{\Delta T}{\Delta e} \tag{B.6}$$

Therefore, to determine Q_H and Q_E over an extensive surface, with accurate measurements of Q^*, Q_G, and profiles of temperature and humidity, the following equations can be used.

$$Q_E = \frac{Q^* - Q_G}{1+\beta} \tag{B.7}$$

$$Q_H = \frac{\beta\ (Q^* - Q_G)}{1+\beta} \tag{B.8}$$

Q_H can also be evaluated as $Q_H = \beta Q_E$.

The Aerodynamic Approach

The aerodynamic method applies under the following conditions:

- neutral stability
- steady state
- constancy of fluxes with height
- similarity of all transfer coefficients

Under these conditions, the plot of wind speed $\mu(z)$ versus the natural logarithm of height $ln(z)$ is linear. Assuming that the slope is constant and equal to μ^*/k, the equation describing the relationship can be written as:

$$\mu(z) = \frac{\mu^*}{k} \ln \frac{z}{z_o} \tag{B.9}$$

where μ^* is the friction velocity ($kz(\partial\mu/\partial z)$) and k is von Karmon's constant (0.4). z_o is the roughness length (y intercept) and can be expressed as:

$$z_o = e^{\ln(\bar{z}) - \left(\frac{\ln(z_2) - \ln(z_1)}{\mu_2 - \mu_1}\right)(\mu(\bar{z}))} \qquad \text{(B.10)}$$

where $\bar{z}$ is the geometric mean height.

Over vegetated surfaces, the slope between wind speed and height becomes non-linear. To overcome this, the surface is displaced to a height at some distance above the actual surface. This new height is called the zero plane displacement (d) and is a function of vegetation height. Therefore, for wind profile measurements taken over vegetation, z must be replaced by (z-d).

Assuming that the turbulent transfer coefficients are equal, Q_E and Q_H can be determined by the following:

$$Q_E = - \frac{\rho c_p}{\gamma} k^2 \left(\frac{\partial \mu}{\partial \ln z}\right)\left(\frac{\partial e}{\partial \ln z}\right) \qquad \text{(B.11)}$$

$$Q_H = - \rho c_p k^2 \left(\frac{\partial \mu}{\partial \ln z}\right)\left(\frac{\partial T}{\partial \ln z}\right) \qquad \text{(B.12)}$$

where $\partial\mu/\partial\ln z$, $\partial e/\partial\ln z$, and $\partial T/\partial\ln z$ are the slopes of the wind speed, vapour pressre and temperature gradients with the natural logarithm of height for the five measurement levels.

These are only valid under conditions of neutral atmospheric stability.

The Richardson Number (Ri) is a convenient index for categorizing atmospheric stability in lower layers of the atmosphere. It is described by:

$$Ri = \frac{g}{\overline{T}} z \cdot \frac{(\partial T/\partial \ln z)}{(\partial \mu/\partial \ln z)^2} \qquad \text{(B.13)}$$

where g is acceleration due to gravity and $\overline{T}$ is in °K and z is the geometric mean height. Ri is a dimensionless number which relates the relative roles of buoyancy (numerator) to mechanical (denominator) forces.

In unstable conditions, the free forces dominate and Ri is a negative number, in an inversion (stable) condition, Ri is positive and $Ri \to 0$ during neutral conditions. Since the above equations apply only to neutral conditions, the following stability functions must be applied. For a stable atmosphere:

$$\Phi_C = \Phi_H = \Phi_W = \Phi_M = (1 - 5Ri)^{-1} \qquad \text{(B.14)}$$

and for an unstable atmosphere:

$$\Phi_H = \Phi_W = \Phi_C = (1 - 16Ri)^{-0.5} \qquad \text{(B.15)}$$

$$\Phi_M = (1 - 16Ri)^{-0.25} \qquad \text{(B.16)}$$

where Φ_H, Φ_W, Φ_M, and Φ_C are dimensionless stability functions for heat, water vapour,

momentum and carbon dioxide, respectively. Equations B.11 and B.12 may now be written as:

$$Q_E = - \frac{\rho c_E}{\gamma} k^2 \left(\frac{\partial \mu}{\partial \ln z} \cdot \frac{\partial e}{\partial \ln z} \right) (\Phi_M \Phi_W)^{-1} \qquad \text{(B.17)}$$

$$Q_H = - \rho c_p k^2 \left(\frac{\partial \mu}{\partial \ln z} \cdot \frac{\partial T}{\partial \ln z} \right) (\Phi_M \Phi_H)^{-1} \qquad \text{(B.18)}$$

C)Theory of Stomatal Conductance Measurements

Leaf conductance was measured using a steady state porometer (LI-1600, Li-Cor, Lincoln, Nebraska, U.S.A.). The LI-1600 uses primary measurements to calculate stomatal resistance or conductance. Water loss from a leaf placed in the LI-1600 cuvette is determined by measuring the flow rate of dry air necessary to maintain a constant relative humidity inside the cuvette. Typically, the ambient relative humidity is used as a null-point, and dry air is injected into the cuvette at a rate which is just sufficient to balance the transpirational water flux out of the leaf. This maintains the cuvette relative humidity at the set-point. Stomatal resistance (or conductance) is calculated directly from the measured values of relative humidity, leaf and air temperature and flow rate.

The volumetric flow rate, F ($cm^3\ s^{-1}$) of dry air in the cuvette can be expressed as:

$$F = \left[\frac{T_c}{273.15} + 1\right]\left[\frac{101.3}{P}\right]M \qquad (C.1)$$

where T_c is the cuvette temperature (°C), P is the barometric pressure at the measurement site (kPa) and M is the standard volumetric flow rate of dry air into the cuvette as measured by the LI-1600 mass flow meter ($cm^3\ s^{-1}$). The mass flow meter is calibrated in volumetric units and referenced at standard temperature and pressure conditions.

The leaf transpiration rate, E ($\mu g\ cm^{-2}\ s^{-1}$) is related to the volumetric flow rate by:

$$E = (\rho_c - \rho_a)\frac{F}{A} \qquad \text{(C.2)}$$

where ρ_c is the water vapour density in the cuvette (μg cm^{-3}), ρ_a is the water vapour density in the dry air stream entering the cuvette (μg cm^{-3}) (a constant RH of 2% is assumed) and A is the leaf area (cm^2).

Leaf transpiration can also be expressed in terms of the vapour density gradient between leaf and air divided by the sum of stomatal plus boundary layer diffusive resistances as follows:

$$E = \frac{\rho_l - \rho_c}{r_s + r_b} \qquad \text{(C.3)}$$

Combining Equations C.2 and C.3 and solving for r_s:

$$r_s = \frac{A}{F}\left(\frac{\rho_l - \rho_c}{\rho_c - \rho_a}\right) - r_b \qquad \text{(C.4)}$$

The LI-1600 uses r_b=0.15 s cm^{-1} in Equation C.4 to calculate stomatal resistance. A table giving saturation vapour density as a function of temperature is stored in the LI-1600 memory. The leaf internal atmosphere is assumed to be saturated, so leaf vapour density corresponds to the saturation vapour density at the measured leaf temperature.

The cuvette vapour density is the saturation vapour density at cuvette temperature times the measured relative humidity divided by 100%.

REFERENCES

Amthor, J.S., (1994). Higher plant respiration and its relationships to photosynthesis. In: Schulze, E.-D. and Caldwell, M.M. (eds.), *Ecophysiology of Photosynthesis*, Ecological Studies, Volume 100, Springer-Verlag, Berlin, Heidelberg, pp. 71-101.

Armentano, T.V. and Menges, E.S., (1986). Patterns of change in the carbon balance of organic-soil wetlands of the temperate zone. *Journal of Ecology*, 74: 755-774.

Bacastow, R.B. and Keeling, C.D., (1981). Atmospheric carbon dioxide concentration and the observed airborne fraction, In: Lemon, E.R. (ed.), *CO_2 and Plants. The response of plants to rising levels of atmospheric carbon dioxide*. Westview Press, Boulder, U.S.A., pp. 107-130.

Barnola, J.M., Raynaud, D., Korotkevich, Y.S. and Lorius, C., (1987). Vostok ice core provides 160,000 year record of atmospheric CO_2. *Nature*, 329: 408-414.

Billings, W.D., (1987). Carbon balance of Alaskan tundra and taiga ecosystems: past, present and future. *Quaternary Science Reviews*, 6: 165-177.

Billings, W.D., Peterson, K.M., Shaver, G.R. and Trent, A.W., (1977). Root growth, respiration and carbon dioxide evolution in an arctic tundra soil. *Arctic and Alpine Research*, 9: 129-137.

Billings, W.D., Peterson, K.M. and Shaver, G.R., (1978). Growth, turnover and respiration rates of roots and tillers in tundra communities. In: Tieszen, L.L. (ed.), *Vegetation and Production Ecology of and Alaskan Arctic Tundra*. Springer, New York, pp. 415-434.

Billings, W.D., Luken, J.O., Mortensen, D.A. and Peterson, K.M., (1982). Arctic tundra: a source or sink for atmospheric carbon dioxide in a changing environment? *Oecologia*, 53: 7-11.

Billings, W.D., Luken, J.O., Mortensen, D.A. and Peterson, K.M., (1983). Increasing atmospheric carbon dioxide: possible effects on arctic tundra. *Oecologia*, 58: 286-289.

Blanken, P., (1992). *Vegetation controls on evaporation from a subarctic willow-birch forest*. M.Sc. thesis, Department of Geography, McMaster University, Hamilton, Ontario.

Burton, K.L, Rouse, W.R. and Boudreau, L.D., (1995). Factors affecting the summer carbon dioxide budget of subarctic wetland tundra. (submitted).

Chapin, F.S., III, Miller, P.C., Billings, W.D. and Coyne, P.I., (1980). Carbon and nutrient budgets and their control in coastal tundra. In: Brown, J., Miller, P.C., Tieszen, L. and Bunnell, F.L. (eds.), *An Arctic ecosystem: the coastal tundra at Barrow, Alaska*. Dowden, Hutchinson and Ross, Stroudsburg, Pennsylvania, U.S.A., pp. 458-482.

Conway, T.J., Tans, P., Waterman, L.S., Thoning, K.W., Masarie, K.A. and Gammon, R.H., (1988). Atmospheric carbon dioxide measurements in the remote global troposphere 1981-1984. *Tellus*, 40(B): 81-115.

Coyne, P.I. and Kelly, J.J., (1974). Variations in carbon dioxide across an arctic snowpack during winter. *Journal of Geophysical Research*. 79: 799-802.

Coyne, P.I. and Kelly, J.J., (1975). CO_2 exchange over the Alaskan Arctic tundra: meteorological assessment by an aerodynamic method. *Journal of Applied Ecology*, 12: 587-611.

Coyne, P.I. and Kelly, J.J., (1978). Meteorological assessment of CO_2 exchange over an Alaskan arctic tundra. In: Tieszen, LL (ed.), *Vegetation and production ecology of an Alaskan arctic tundra*. Ecological Studies 19. Springer, Berlin Heidelberg New York, pp. 299-319.

Emanuel, W.R., Shugart, H.H. and Stevenson, M.P., (1985). Response to comment: Climatic change and the broad-scale distribution of terrestrial ecosystem complexes. *Climatic Change*, 7: 457-460.

Flanagan, P.W. and Veum, A.K., (1974). Relationships between respiration, weight loss, temperature and moisture in organic residues on tundra. In: Holding, A.J., Heal, O.W., MacLean, Jr. S.F. and Flanagan, P.W. (Eds.), *Soil Organisms and Decomposition in Tundra*. Tundra Biomass Steering Committee, Stockholm, pp 249-277.

Friedli, H., Lotscher, H., Oeschger, H., Siegenthaler, U. and Stauffer, B., (1986). Ice core record of $^{13}C/^{12}C$ ratio of atmospheric CO_2 in the past two centuries. *Nature*, 324: 237-238.

Gammon, R.H., Sundquist, E.T. and Fraser, P.J., (1985). History of carbon dioxide in the atmosphere. In: Trabalka, J.R. (ed.), *Atmospheric Carbon Dioxide and the Global Carbon Cycle*, Chapter 2, U.S. Department of Energy, DOE/ER-0239. Washington, D.C., pp. 25-62.

Glenn, M.S., Heyes, A. and Moore, T.R., (1993). Carbon dioxide and methane fluxes from drained pea soils, southern Quebec. *Global Biogeochemical Cycles*, 7: 247-257.

Gorham, E., (1991). Northern peatlands: role in the carbon cycle and probable responses to climatic warming. *Ecological Applications*, 1: 182-195.

Grammerer, K., (1989). *Respiration of soil and vegetation in grassland.* M.S. thesis, Department of Agronomy, University of Nebraska, Lincoln.

Halliwell, D.H., (1989). *A numerical model of the surface energy balance and ground thermal regime in organic permafrost terrain.* Ph.D. thesis, Department of Geography, McMaster University, Hamilton, Ontario, pp. 195.

Halliwell, D.H. and Rouse, W.R., (1987). Soil heat flux in permafrost: characteristics and accuracy of measurement. *Journal of Climatology*, 7: 571-584.

Hayes, J.D., Imbrie, J. and Shackleton, N.J., (1976). Variation in the Earth's orbit: pacemaker of the Ice Ages. *Science*, 194: 1121-1132.

Hilbert, D.W., Prudhomme, T.I. and Oechel W.C., (1987). Responses of tussock tundra to elevated carbon dioxide regimes: analysis of ecosystem CO_2 flux through nonlinear modeling. *Oecologia*, 72: 466-472.

Hogg, E.H., Lieffers, V.J. and Wein, R.W. (1992). Potential carbon losses from peat profiles: effects of temperature, drought cylces, and fire. *Ecological Applications*, 2(3): 298-306.

Intergovernmental Panel on Climate Change, (1990). *Climate Change: The IPCC Scientific Assessment.* Cambridge University Press, Cambridge, pp. 138.

Johnson, L.C. and Damman, A.W.H., (1991). Species-controlled *Sphagnum* decay on a south Swedish raised bog. *Oikos*, 61: 234-242.

Keeling, C.D., (1988). *Overview of Scripps Program to Observe Atmospheric Carbon Dioxide.* Report to Committee on Global Change, National Research Council, Washington, D.C., U.S.A.

Kim, J. and Verma, S.B., (1992). Soil surface CO_2 flux in a Minnesota peatland. *Biogeochemistry*, 18: 37-51.

Kim, J., Verma, S.B. and Clement, R.J., (1992). Carbon dioxide budget in a temperate grassland ecosystem. *Journal of Geophysical Research*, 97(D5): 6057-6063.

Larcher, W., (1980). *Physiological Plant Ecology*. Springer-Verlag, Berlin, Heidelberg, New York, pp. 73-157.

Luken, J.O. and Billings, W.D., (1985). The influence of microtopographic heterogeneity on carbon dioxide efflux from a subarctic bog. *Holarctic Ecology*, 8: 306-312.

Manabe, S. and Stouffer, R.J., (1980). Sensitivity of a global climate model to an increase of CO_2 concentration in the atmosphere. *Journal of Geophysical Research*, 85: 5529-5554.

Mellilo, J.M., Callaghan, T.., Woodward, F.I., Salati, E. and Sinha, S.K., (1990). Effects on ecosystems. In: Houghton, J.T., Jenkins, G.J. and Ephraums, J.J. (eds.), *Climate Change: the IPCC Scientific Assessment.* Cambridge: Cambridge University Press, pp. 283-310.

Miller. P.C., (1981). *Carbon dioxide effects research and assessmnet program: Carbon balance in northern ecosystems and potential effect of carbon dioxide induced climatic change*. Report of a workshop, San Diego, California, March 7-9, 1980. Washington D.C.: U.S. Department of Energy, CONF-8003118, pp. 109.

Miller, P.C. Kendall, R. and Oechel, W.C., (1983). Simulating carbon accumulation in northern ecosystems. *Simulation*, 40: 119-141.

Minstry of Supply and Service, (1991). *Climatic change: warming to the challenge*. The State of the Environment Report No. 22, Ottawa, pp. 28.

Mogensen, V.O., (1977). Field measurements of dark respiration rates of roots and aerial parts in Italian ryegrass and barley. *Journal of Applied Ecology*, 14: 243-252.

Moore, T.R., (1986). Carbon dioxide evolution from subarctic peatlands in eastern Canada. *Arctic and Alpine Research*, 18: 189-193.

Moore, T.R., (1989). Plant production, decomposition, and carbon efflux in a subarctic patterned fen. *Arctic and Alpine Research*, 21(2): 156-162.

Moore, T.R. and Knowles, R., (1989). The influence of water table levels on methane and carbon dioxide emissions from peatland soils. *Canadian Journal of Soil Science*, 69: 33-38.

Neftel, A., Oeschger, H., Schwander, J., Stauffer, B. and Zumbrunn, R., (1982). Ice core sample measurements give atmosphere CO_2 content during the past 40,000 years. *Nature*, 295: 220-223.

Neftel, A., Moor, E., Oeschger, H. and Stauffer, B., (1985). The increase of atmospheric CO_2 in the last two centuries. *Nature*, 315: 45-47.

Neumann, H.H., den Hartog, G., King, K.M. and Chipanshi, A.C., (1994). Carbon dioxide fluxes over a raised open bog at Kinosheo Lake tower site during the Northern Wetlands study (NOWES). *Journal of Geophysical Research*, 99(D1): 1529-1538.

Norman, J.M., Garcia, R.and Verma, B., (1992). Soil surface CO_2 fluxes and the carbon budget of a grassland. *Journal of Geophysical Research*, 97(D17): 18,845-18,853.

Oechel, W.C., Hastings, S.J., Vourlitis, G., Jenkins, M., Reichers, G. and Grulke, N., (1993). Recent change of Arctic tundra ecosystems from a net carbon dioxide sink to a source. *Nature*, 361: 520-523.

Oberbauer, S.F., Tenhunen, J.D. and Reynolds, J.F., (1991). Environmental effects on CO_2 efflux from water track and tussock tundra in Arctic Alaska, U.S.A. *Arctic and Alpine Research*, 23: 162-169.

Oberbauer, S.F., Gillespie, C.T., Cheng, W., Gebauer, R., Sala Serra, A. and Tenhunen, J.D., (1992). Environmental effects on CO_2 efflux from riparian tundra in the northern foothills of the Brooks Range, Alaska, USA. *Oecologia*, 92: 568-577.

Oke, T.R., (1987). *Boundary Layer Climates*, 2nd Edition, Routledge, New York, pp. 435.

Pate, J.S. and Layzell, D.B., (1990). Energetics and biological costs of nitrogen assimilation. *Biochemistry of Plants*, 16: 1-42.

Pearman, G.I. and Hyson, P. (1980). Activities of the global biosphere as reflected in atmospheric CO_2 records. *Journal of Geophysical Research*. 85: 4457-4467.

Peterson, K.M. and Billings, W.D., (1975). Carbon dioxide flux from tundra soils and vegetation as related to temperature at Barrow, Alaska. *The American Midland Naturalist*, 94: 88-98.

Peterson, K.M., Billings, W.D. and Reynolds, D.N., (1984). Influence of water table and atmospheric CO_2 concentration on the carbon balance of arctic tundra. *Arctic and Alpine Research*, 16: 331-335.

Poole, D.K. and Miller, P.C., (1982). Carbon dioxide flux from three arctic tundra types in north-central Alaska, U.S.A., *Arctic and Alpine Research*, 14(1): 27-32.

Post, W.M., Emanuel, W.R., Zinke, P.J. and Stangenberger, A.G., (1982). Soil carbon pools and world life zones. *Nature*, 298: 156-159.

Rosenburg, N.J., Blad, B.L. and Verma, S.B., (1983). *Microclimate: The Biological Environment*, 2nd Edition, John Wiley, New York, pp. 495.

Rotty, R.M. and Masters, C.D., (1985). Carbon dioxide from fossil fuel combustion: trends, resources, and technological implications. In: Trabalka, J.R. (ed.), *Atmospheric Carbon Dioxide and the Global Carbon Cycle*, U.S. Department of Energy, DOE/ER-0239, Washington, D.C., pp. 63-80.

Solomon, A.M., Trabalka, J.R., Reichle, D.E. and Voorhees, L.D., (1985). The global cycle of carbon. In: Trabalka, J.R. (ed.), *Atmospheric Carbon Dioxide and the Global Carbon Cycle*, U.S. Department of Energy, DOE/ER-0239, Washington, D.C., pp. 1-13.

Stewart, J.M. and Wheatley, R.E., (1990). Estimates of CO_2 production from eroding peat surfaces. *Soil Biological Biochemistry*, 22: 65-68.

Svensson, B.H., (1980). Carbon dioxide and methane fluxes from the ombrotrophic parts of a subarctic mire. *Ecological Bulletin*, 30: 235-250.

Tarnocai, C., (1984). *Peat resources of Canada*. Land Resource Research Institute, Research Branch, Agriculture Canada, Ottawa, Ontario, Canada.

Tieszen, L.L., (1978). *Vegetation and Production Ecology of an Alaskan Arctic Tundra*. Springer, New York.

Trabalka, J.R. (ed.), (1985). *Atmospheric Carbon Dioxide and the Global Carbon Cycle*. U.S. Department of Energy, DOE/ER-0239, Washington, D.C.

Webb, E.K., Pearman, G.I. and Leuning, R., (1980). Corrections of flux measurements of density effects due to heat and water vapour transfer. *Quarterly Journal of the Royal Meteorological Society*, 106: 85-100.

Whiting, G.J., Bartlett, D.S., Fan, S., Bakwin, P.S. and Wofsy, S.C., (1992). Biosphere/atmosphere CO_2 exchange in tundra ecosystems: community characteristics and relationships with multispectral surface reflectance. *Journal of Geophysical Research*, 97(D15): 16,671-16,680.

Zoltai, S.C., Pollett, F.C., Jeglum, J.K. and Adams, G.D., (1973). Developing a wetland classification for Canada. In: *Proceedings of the 4th North American Forest Soils Conference*, pp. 497-511.

Zoltai, S.C. and F.C. Pollett, (1983). Wetlands in Canada: their classification, distribution and use. In: Gore, A.J.P. (ed.), *Mires: swamp, bog, fen and moor*. Elsevier Scientific Publishing Company, New York, pp. 245-267.